Convective Modes for Significant Severe Thunderstorms in the Contiguous United States. Part I: Storm Classification and Climatology

BRYAN T. SMITH, RICHARD L. THOMPSON, JEREMY S. GRAMS, AND CHRIS BROYLES

NOAA/NWS/NCEP/Storm Prediction Center, Norman, Oklahoma

HAROLD E. BROOKS

NOAA/National Severe Storms Laboratory, Norman, Oklahoma

(Manuscript received 4 October 2011, in final form 22 March 2012)

ABSTRACT

Radar-based convective modes were assigned to a sample of tornadoes and significant severe thunderstorms reported in the contiguous United States (CONUS) during 2003–11. The significant hail (≥2-in. diameter), significant wind (≥65-kt thunderstorm gusts), and tornadoes were filtered by the maximum event magnitude per hour on a 40-km Rapid Update Cycle model horizontal grid. The filtering process produced 22 901 tornado and significant severe thunderstorm events, representing 78.5% of all such reports in the CONUS during the sample period. The convective mode scheme presented herein begins with three radar-based storm categories: 1) discrete cells, 2) clusters of cells, and 3) quasi-linear convective systems (QLCSs). Volumetric radar data were examined for right-moving supercell (RM) and left-moving supercell characteristics within the three radar reflectivity designations. Additional categories included storms with marginal supercell characteristics and linear hybrids with a mix of supercell and QLCS structures. Smoothed kernel density estimates of events per decade revealed clear geographic and seasonal patterns of convective modes with tornadoes. Discrete and cluster RMs are the favored convective mode with southern Great Plains tornadoes during the spring, while the Deep South displayed the greatest variability in tornadic convective modes in the fall, winter, and spring. The Ohio Valley favored a higher frequency of QLCS tornadoes and a lower frequency of RM compared to the Deep South and the Great Plains. Tornadoes with nonsupercellular/non-QLCS storms were more common across Florida and the high plains in the summer. Significant hail events were dominated by Great Plains supercells, while variations in convective modes were largest for significant wind events.

1. Introduction

Our understanding of the convective mode has increased considerably in the past few decades, beginning with the pioneering work by Browning (1964) documenting conventional radar observations and inferred airflow within supercell thunderstorms, continuing with descriptions of organized bow echoes (Fujita 1978), and a host of more recent studies (e.g., Weisman and Trapp 2003; Trapp and Weisman 2003) examining quasi-linear convective systems (QLCSs). Convective mode is widely recognized as an important contributor to the likelihood and type of severe convective weather (e.g., tornadoes, large hail, damaging wind gusts). Prior work by Trapp et al. (2005, hereafter T05) considered a relatively simple designation of the convective mode for 3828 tornadoes in the contiguous United States (CONUS) from 1999 to 2001. They used regional radar mosaics of base-elevation reflectivity, and did not attempt to specify convective mode beyond a QLCS, cell, or ''other'' classification scheme. Grams et al. (2012) followed a similar scheme in classifying convective mode for 448 significant tornado events in the CONUS from 2000 to 2008. Gallus et al. (2008, hereafter G08) employed a more detailed radar reflectivity classification scheme (nine distinct convective morphologies). Like T05, G08 examined regional radar reflectivity mosaics every 30 min for 949 cases of documented convective mode, and associated all severe reports with a storm type over the Great Plains and Upper Midwest during the 2002 warm season. More recent work by Duda and Gallus (2010) considered the

Corresponding author address: Bryan T. Smith, NOAA/NWS/NCEP/Storm Prediction Center, Ste. 2300, 120 David L. Boren Blvd., Norman, OK 73072.
E-mail: bryan.smith@noaa.gov

DOI: 10.1175/WAF-D-11-00115.1

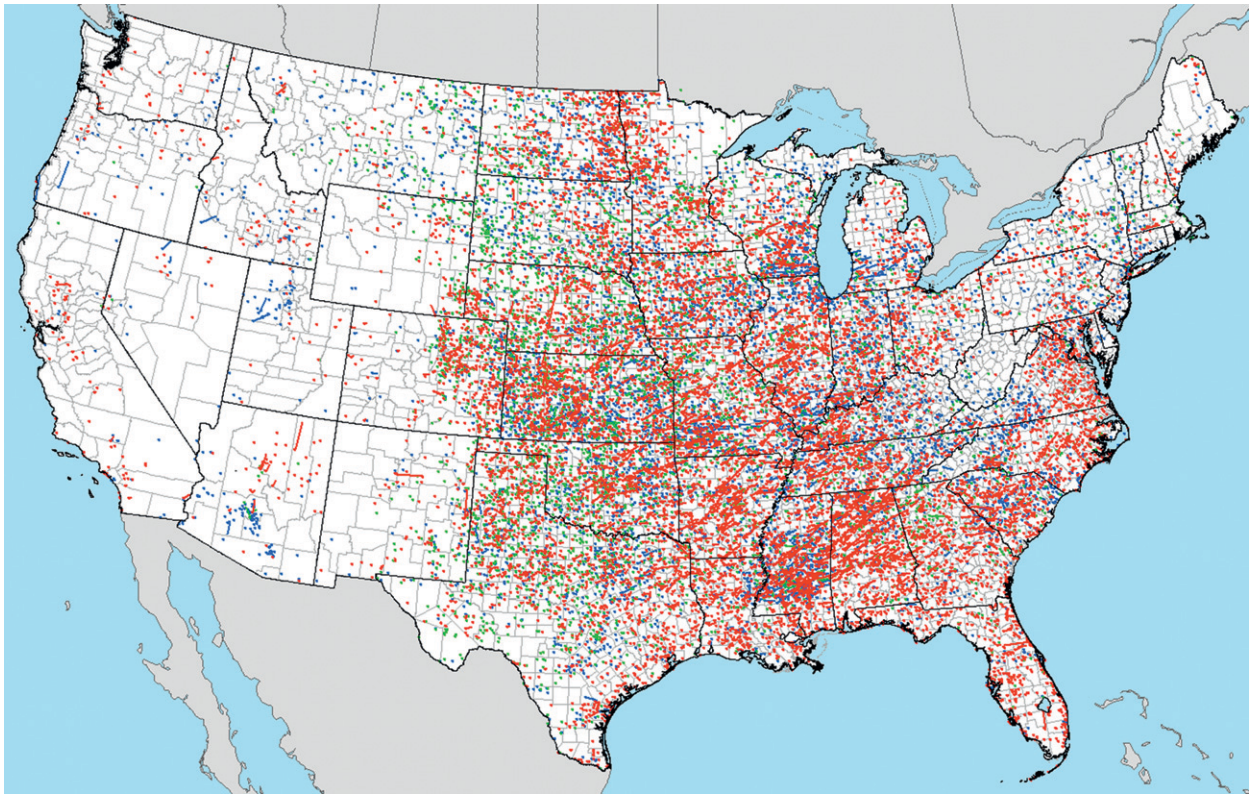

FIG. 1. All tornado (red), sighail (green), and sigwind (blue) events filtered for the largest magnitude event per hour of each type on a 40-km grid for the period 2003–11.

same nine convective morphologies and geographic region as G08, except they examined storms during the 2007 warm season (909 cases of documented convective mode) and included supercell identification based on explicit output from the Weather Surveillance Radar-1988 Doppler (WSR-88D) mesocyclone detection algorithm (MDA) described by Stumpf et al. (1998). Their supercell identifications relied on consecutive volume scans of the MDA output exceeding a certain threshold and also required a cellular convective morphology.

The aforementioned studies dealt with classification schemes, some of which were relatively simple, based primarily on regional radar mosaics of base-elevation reflectivity with rather coarse spatial (2–8 km) and temporal (30 min) resolutions. Archival of WSR-88D data began in the early to mid-1990s (Crum et al. 1993) and, until recently, detailed individual radar convective mode climatologies have not been possible. Studies such as Hocker and Basara (2008a,b) and Smith et al. (2008) utilized full WSR-88D volumetric data (base reflectivity and velocity at multiple elevation scans updated every 5 min), but for only state or regional investigations of convective mode and resultant spatial–temporal evolutions of supercells or QLCS. Kis and Straka (2010, hereafter KS10) utilized WSR-88D reflectivity data to classify a sample of 69 nocturnal tornadoes from 29 event days in the CONUS from 2004 to 2006 into supercells and circulations embedded within or adjacent to mesoscale convective systems, including QLCSs.

This study complements and enhances results from past convective mode investigations by increasing the number of radar-recognizable storm classifications using volumetric WSR-88D level II data for a very large sample of severe thunderstorm and tornado events. Following Hales (1988), we focus our efforts on tornadoes and significant severe reports [i.e., estimated or measured ≥2-in. (5.04 cm) diameter hail (hereafter sighail) and ≥65 kt (33.4 m s^{-1}) convective wind gusts (hereafter sigwind)] since they often result in a disproportionate threat to life and property.

Part II of this overall study (Thompson et al. 2012, this issue) examines relationships between severe thunderstorm events, convective mode, and environmental conditions using Storm Prediction Center (SPC) hourly mesoanalysis data (Bothwell et al. 2002; Schneider and Dean 2008). Edwards et al. (2012, hereafter Part III) investigate the convective mode and environmental data with a focus on tropical cyclone tornadoes.

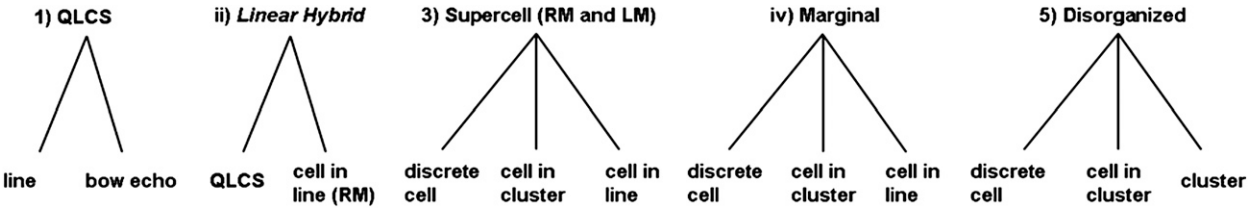

FIG. 2. Convective mode decision tree.

2. Data and methods

a. Data and event filtering

All tornado, sighail, and sigwind reports for the period 2003–11 were filtered for the largest magnitude report per hour (based on the initial time of the report) on a Rapid Update Cycle (RUC) model (Benjamin et al. 2004) analysis grid with 40-km horizontal grid spacing. Tornado segment data (i.e., tornado damage paths broken down by individual tornadoes and counties) were used in response to long-track tornadoes that crossed multiple grid boxes and/or hours. This filtering procedure produced a sample of 22 901 severe thunderstorm grid-hour events, including 10 753 tornadoes (77% of all county tornado segments), 4653 sighail events (79% of all sighail), and 7495 sigwind events (81% of all sigwind) during the 9-yr period (Fig. 1). Subsignificant hail/wind events or null cases (i.e., storms without severe weather reports) were not considered due to the difficulty of subjective case identification associated with what would be an overwhelming sample size.

Numerous studies have highlighted limitations and biases in severe convective wind reports in the National Climatic Data Center (NCDC) publication *Storm Data*. Some of these include (i) overestimated wind speeds by human observers (Doswell et al. 2005), (ii) a largely secular (nonmeteorological) increase in the number of reports (Weiss et al. 2002), and (iii) the dependence of report frequencies on population density and time of day (Trapp et al. 2006). Similar issues impact tornado reports (e.g., Doswell and Burgess 1988). These caveats associated with the severe report database are acknowledged but we made no attempts to adjust the reported event magnitudes. However, careful temporal or spatial adjustments were made to a small portion (4.3%) of the event database. A large majority of suspected report errors involved incorrectly listed report times when event times were compared to radar data. Examples of this error type included reports well removed from existing convection and time differences on the order of tens of minutes to an hour or more. Offsets of 1 h were relatively common near time zone boundaries, although a few reports required extensive investigation to identify likely errors of up to several days. In situations where a suspected error could not be easily corrected, *Storm Data* was used to examine the questionable report's narrative description in an effort to identify the storm responsible for the event.

b. Radar-based storm mode classification criteria

Archived level II WSR-88D data from NCDC (http://www.ncdc.noaa.gov/nexradinv/) were utilized from the closest radar site[1] to an event (up to 230 km) to assign one of the following major convective mode classes (Fig. 2) for each severe thunderstorm event: QLCS, supercell, and disorganized (cells and clusters clearly not achieving QLCS or supercell criteria). Subclassifications of each major category were as follow: QLCS included well-defined bow echo and line (e.g., extensive squall lines, or smaller-scale convective line segments); right-moving (cyclonic) supercells (RMs) or left-moving (anticyclonic) supercells (LMs) included discrete cell, cell in cluster, and cell in line; and disorganized included discrete cell, cell in cluster, and cluster. Additionally, two other minor classifications were noted: storms with marginal supercell characteristics (after Thompson et al. 2003), and linear hybrid modes with a mix of QLCS and line RM characteristics [see later discussion in section 3a(c)]. Additionally, storm events associated with tropical cyclones (TCs) were documented.

This classification scheme can be compared to that used by G08 (their Fig. 2) as follows (G08 in parentheses): discrete cell (isolated cell), cell in cluster (cell cluster), cell in line (broken line, length-scale dependent), QLCS with bow echo as a subset (five linear modes), and cluster (NL). The current convective mode categories can also be simplified to match T05, where their ''other'' category includes disorganized storm cells and clusters.

A subjective reflectivity threshold of 35 dBZ was used for storm identification, with cells consisting of discrete areas of above-threshold reflectivity generally containing a single dominant updraft. QLCS events consist of contiguous reflectivity at or above the threshold for a

[1] Level III archived data were used when level II data were missing, or when a site with only level III archived data provided superior resolution of an event.

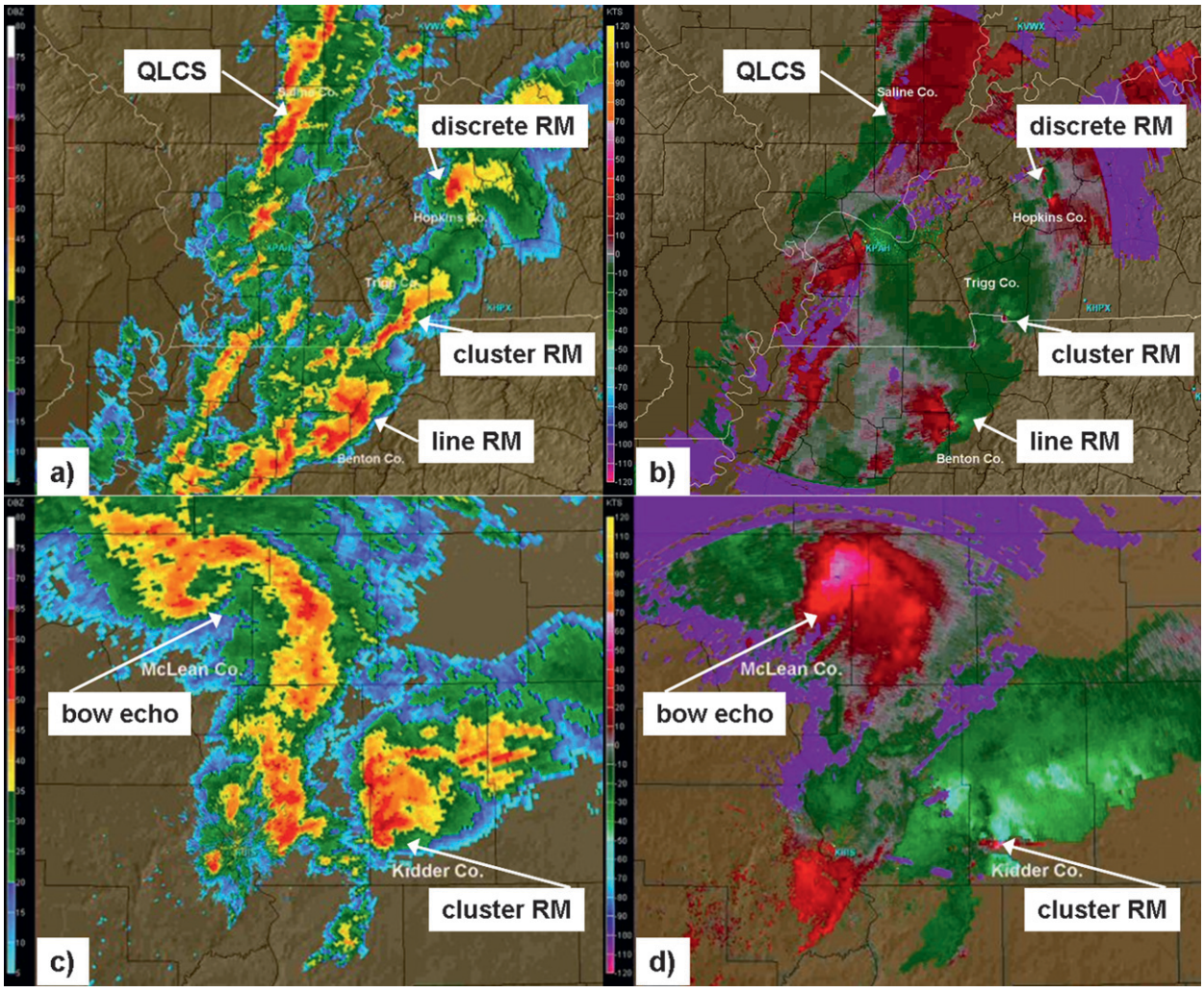

FIG. 3. (a),(c) WSR-88D base reflectivity and (b),(d) storm relative velocity at 0.5° beam tilt. Radar imagery displayed in (a),(b) from Paducah, KY (KPAH), at 2132 UTC 15 Nov 2005 (dB*Z* and kt, color scale on left). A discrete RM produced an EF4 tornado in Hopkins County, KY (start time 2127 UTC), and EF0 tornado and sigwind reports occurred with the QLCS in Saline County, IL (2132 UTC); a cluster RM in Trigg County, KY (2135 UTC); and a line RM in Benton County, TN, that produced EF1 and EF2 tornadoes at 2135 and 2138 UTC, respectively. Radar imagery displayed in (c),(d) is from Bismarck, ND (KBIS), at 1956 UTC on 24 Aug 2006. A cluster RM produced an EF0 tornado in Kidder County, ND (report start time is 2003 UTC). The bow echo in McLean County, ND, was responsible for an EF2 tornado (1855 UTC) and two sigwind events (1920 and 1945 UTC). North is up, state (county) borders are white (black), and radar locations are labeled in cyan.

horizontal distance of at least 100 km and a length-to-width aspect ratio of at least 3 to 1 at the time of the event, similar to T05. Clusters were conglomerates of storms meeting the reflectivity threshold but not satisfying either cell or QLCS criteria.

The Gibson Ridge radar viewers (http://www.grlevelx.com/) were used to analyze archived WSR-88D level II or level III single-site radar data. Convective mode was determined using the volume scan immediately prior to reported severe event time. Full volumetric radar data were used to determine the convective mode of each event. Only after the major and minor convective mode categorization (i.e., supercell, QLCS, disorganized; marginal supercell, linear hybrid) was determined was preference given to the lowest elevation tilt (i.e., 0.5°) of base reflectivity to classify storms into subcategories (i.e., discrete cell, cell in cluster, cell in line, cluster). Secondary emphasis was then given to subsequent higher tilts of radar data if the lowest tilt was unavailable (e.g., range folded or improperly dealiased velocity data), or when data through a deep layer were needed to perform a more thorough assessment of storm structure. If level II data were unavailable, then level III data were used. In situations where radar data were unavailable or incomplete, convective mode was not assigned (0.30% of total cases).

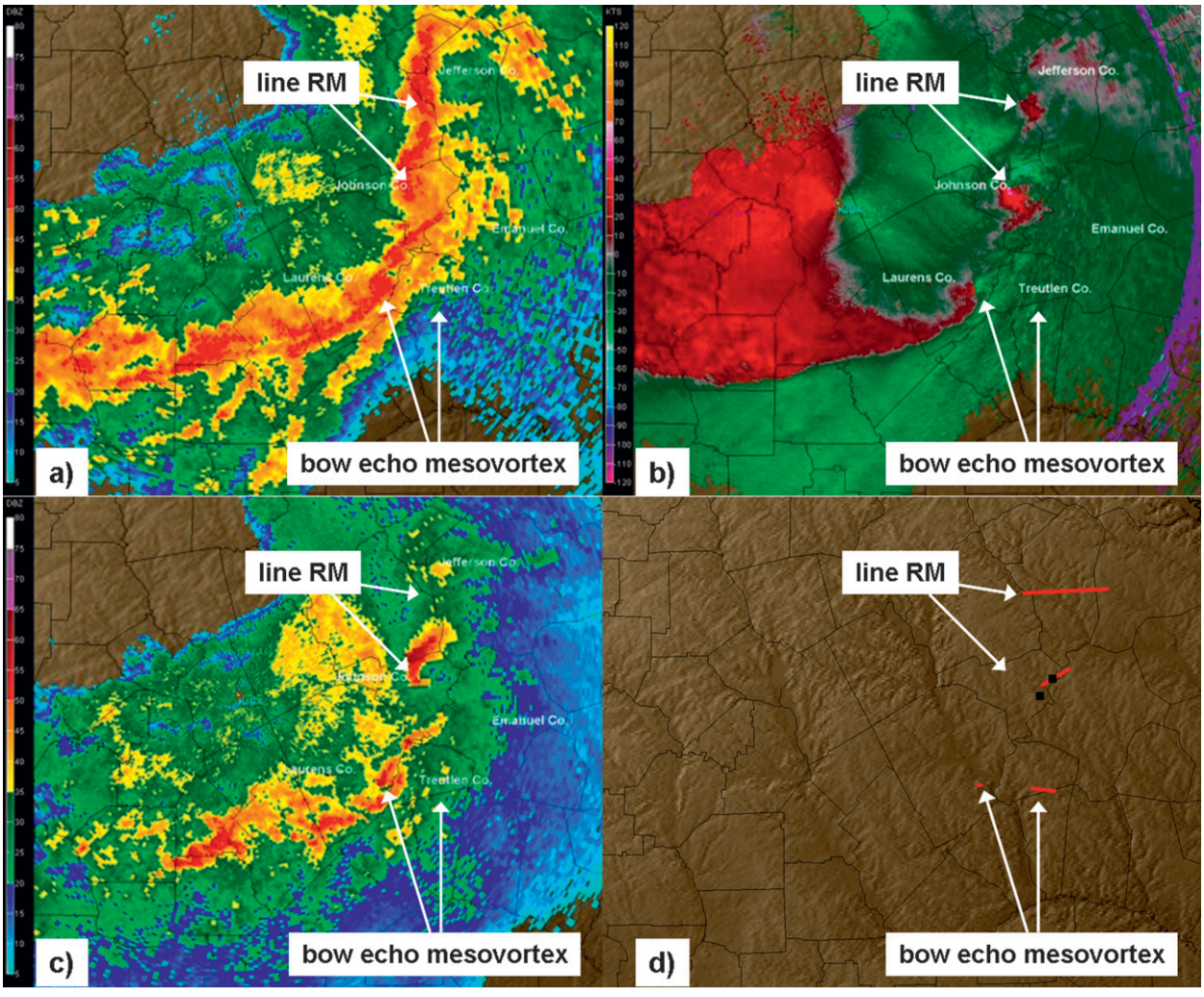

FIG. 4. (a) WSR-88D base reflectivity and (b) storm-relative velocity 0.5° beam tilt from Robins AFB, GA (KJGX), at 1057 UTC 11 May 2008. (c) Base reflectivity from a 3.9° beam tilt sampling of the Johnson County line RM near 17 000 ft (5.18 km) AGL. (d) Red lines (tornado) and black squares (sigwind) denote event locations. A line RM in GA produced an EF0 tornado in Jefferson County (report start time is 1057 UTC), an EF0 tornado was associated with the bow-echo mesovortex in Laurens County (1058 UTC), a line RM produced an EF2 tornado and sigwind events in Johnson County (1101 UTC), a line RM produced an EF2 tornado and sigwind events in Emanuel County (1107 UTC), and an EF3 tornado was produced by a bow-echo mesovortex in Treutlen County (1111 UTC). All events described herein were considered linear hybrids. Same label conventions are as in Fig. 3.

Discrete or embedded cells with focused areas of cyclonic (or anticyclonic) azimuthal shear were further scrutinized as potential supercells, following the mesocyclone nomograms developed by the Warning Decision Training Branch of the National Weather Service (NWS; after Andra 1997; Stumpf et al. 1998). Supercells required a peak rotational velocity $\geq$10 m s^{-1} [i.e., a peak-to-peak azimuthal velocity difference of roughly 20 m s^{-1} over a distance of less than ~7 km, or 3.5 nautical miles (n mi)], rotation $\geq$¼ the depth of the storm, and rotation duration of at least 10–15 min. Range dependence was included in the mesocyclone designation, per the 1-, 2-, and 3.5-n mi mesocyclone nomograms. Circulations were classified as weak shear (nonsupercell), and weak, moderate, or strong supercells, following the range-dependent horizontal peak rotational velocity values of the mesocyclone nomograms. Storms that exhibited persistent, weak azimuthal shear just below the nomogram's minimal mesocyclone threshold and transient supercell reflectivity structure, or identifiable rotation (regardless of magnitude) for no more than two consecutive volume scans (i.e., <10 min), were binned in the marginal supercell category. Other tornadic storms not displaying QLCS, linear hybrid, supercell, or marginal supercell criteria were assigned to the disorganized category as either discrete cell, cell in cluster, or cluster based on lowest elevation angle reflectivity structure.

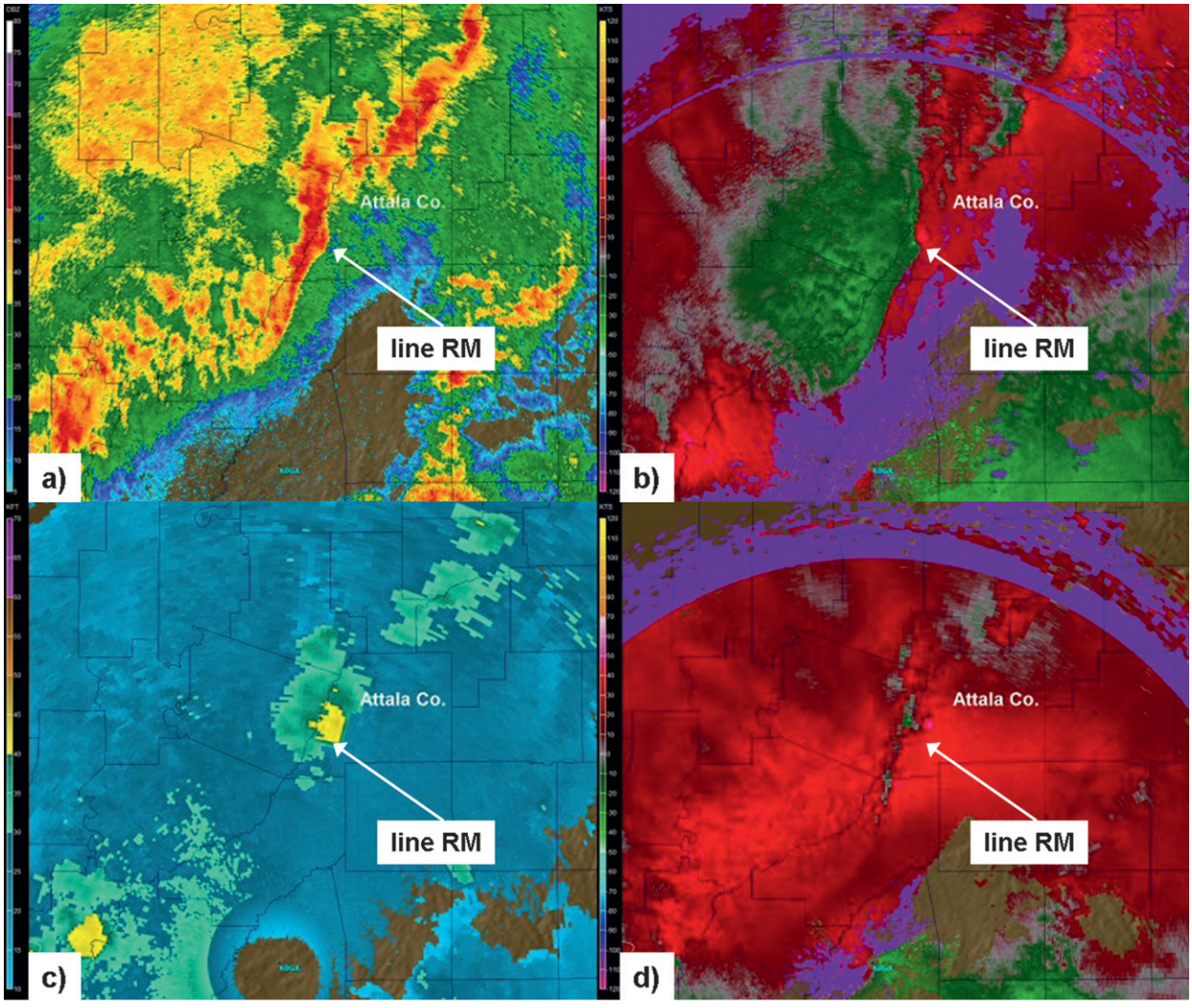

FIG. 5. (a) WSR-88D base reflectivity and (b) storm-relative velocity 0.5° beam tilt from KDGX at 0127 UTC 10 Dec 2008. (c) Echo-top height and (d) storm-relative velocity at 3.2° beam tilt when sampling the Attala County, MS, line RM near 18 000 ft (5.49 km) AGL. A line RM produced an EF1 tornado (0127 UTC) and sigwind event (0133 UTC) in Attala County. Same label conventions are as in Fig. 3.

The application of this mode classification scheme provided results that were conceptually similar to most previous mode studies, with a notable difference being that the current sample is considerably larger in size and covers a much larger geographic domain. An exception was the KS10 study of nocturnal tornadoes, which found that nearly all events in their relatively small sample were associated with QLCS mode. This finding appears to be caused by the use of a different radar definition that did not include contiguous reflectivity as part of their QLCS criteria. As such, a series of discrete cells were often classified as lines in their study. For instance, what KS10 classified as a broken line of cells and a cell on the southern end of a QLCS as shown in their Figs. 3b and 3c were classified as discrete RMs in the current study, given the lack of any continuous radar reflectivity. Striking differences were noted for these two categories when comparing 65 of their cases to our classifications (4 cases were removed due to the filtering described in section 2a). Of the 26 broken line of cells classified in KS10, our study identified 13 of these events as discrete RMs, 10 as line RMs, and 3 as cluster RMs. Of the four cells on the southern end of a QLCS in KS10, three were discrete RMs and one was a cluster RM in our study. KS10 noted that 61 of their 69 significant nocturnal tornadoes occurred in QLCS. Our classification scheme identified only 9 of the 65 common cases as QLCS, with 20 as line RM.

c. Spatial event distribution and grid smoothing

Although this dataset includes thousands of event types by convective mode, our sample is necessarily

TABLE 1. Tornado, sighail, and sigwind event counts (relative frequency in parentheses) by convective mode category. Relative frequencies are highlighted in the following manner: <0.100, regular font; 0.100–0.249, italic; 0.250–0.499, boldface; and ≥0.500, boldface italic.

Mode	Tornado	Sighail	Sigwind
Total events	10 753	4653	7495
Assigned mode	10 724 (1.000)	4625 (1.000)	7483 (1.000)
Discrete RM	3089 (**0.288**)	2112 (**0.457**)	610 (0.082)
Cluster RM	3378 (**0.315**)	1562 (**0.338**)	1127 (*0.151*)
Line RM	1202 (*0.112*)	236 (0.051)	449 (0.060)
Discrete LM	22 (0.002)	296 (0.064)	71 (0.009)
Cluster LM	13 (0.001)	211 (0.046)	62 (0.008)
Line LM	0 (0.000)	13 (0.003)	3 (0.000)
Discrete or cluster RM + LM	6502 (***0.606***)	4181 (***0.904***)	1870 (**0.250**)
All RM	7669 (***0.715***)	3910 (***0.845***)	2186 (**0.292**)
All LM	35 (0.003)	520 (*0.112*)	136 (0.018)
All RM + LM	7704 (***0.718***)	4430 (***0.958***)	2322 (**0.310**)
Linear hybrid (subset line RM + QLCS)	294 (0.027)	3 (0.001)	173 (0.023)
Bow echo (subset QLCS)	212 (0.020)	7 (0.002)	689 (0.092)
QLCS	1484 (*0.138*)	37 (0.008)	2843 (**0.380**)
Linear (QLCS + line RM or LM + line marginal)	2716 (**0.253**)	295 (0.064)	3316 (**0.443**)
Marginal supercell	354 (0.033)	75 (0.016)	178 (0.024)
Disorganized	1182 (*0.110*)	82 (0.018)	2140 (**0.286**)
No data	29 (0.003)	28 (0.006)	12 (0.002)

incomplete, and likely unrepresentative of a much longer period of time, since it covers only 9 yr. A spatial smoother was employed to account for shortcomings in our sampling of severe storm events, and to provide a preliminary climatological estimate of severe event and convective mode distributions. A kernel density estimation tool using ESRI ArcGIS ArcMap Spatial Analyst extension software was utilized to examine the convective mode by event type on a 40-km horizontal grid, using a quadratic kernel function [Silverman 1986, his Eq. (4.5)] that decays to zero at 400 km. For the sake of consistency, all kernel density estimates used herein matched the horizontal grid resolution (i.e., 40 km) used for environment assessment (see Thompson et al. 2012).

3. Mode classification difficulties and challenges

Given the observed complexity of convective storm initiation, evolution, and decay, it should not be surprising that storms did not always fit cleanly into

TABLE 2. Tornado event count (relative frequency in parentheses) by EF-scale damage for each convective mode category. Other conventions are as in Table 1.

Mode	EF0+	EF1+	EF2+	EF3+	EF4+
Total events	10 753	4645	1480	431	89
Assigned mode	10 724 (1.000)	4634 (1.000)	1479 (1.000)	431 (1.000)	89 (1.000)
Discrete RM	3089 (**0.288**)	1356 (**0.293**)	572 (**0.387**)	207 (**0.480**)	52 (***0.584***)
Cluster RM	3378 (**0.315**)	1545 (**0.333**)	518 (**0.350**)	164 (**0.381**)	33 (**0.371**)
Line RM	1202 (*0.112*)	702 (*0.151*)	221 (*0.149*)	48 (*0.111*)	4 (0.045)
Discrete LM	22 (0.002)	4 (0.001)	0 (0.000)	0 (0.000)	0 (0.000)
Cluster LM	13 (0.001)	6 (0.001)	0 (0.000)	0 (0.000)	0 (0.000)
Line LM	0 (0.000)	0 (0.000)	0 (0.000)	0 (0.000)	0 (0.000)
Discrete or cluster RM + LM	6502 (***0.606***)	2911 (***0.628***)	1090 (***0.737***)	371 (***0.861***)	85 (***0.955***)
All RM	7669 (***0.715***)	3603 (***0.778***)	1311 (***0.886***)	419 (***0.972***)	89 (***1.000***)
All LM	35 (0.003)	10 (0.002)	0 (0.000)	0 (0.000)	0 (0.000)
All RM + LM	7704 (***0.718***)	3613 (***0.780***)	1311 (***0.886***)	419 (***0.972***)	89 (***1.000***)
Linear hybrid (subset line RM + QLCS)	294 (0.027)	193 (0.042)	53 (0.036)	10 (0.023)	1 (0.011)
Bow echo (subset QLCS)	212 (0.020)	148 (0.032)	47 (0.032)	5 (0.012)	0 (0.000)
QLCS	1484 (*0.138*)	802 (*0.173*)	152 (*0.103*)	11 (0.026)	0 (0.000)
Linear (QLCS + line RM + line marginal)	2716 (**0.253**)	1513 (**0.326**)	376 (**0.254**)	59 (*0.137*)	4 (0.045)
Marginal supercell	354 (0.033)	69 (0.015)	8 (0.005)	0 (0.000)	0 (0.000)
Disorganized	1182 (*0.110*)	150 (0.032)	8 (0.005)	1 (0.002)	0 (0.000)
No data	29 (0.003)	11 (0.002)	1 (0.001)	0 (0.000)	0 (0.000)

TABLE 3. Mesocyclone strength by tornado F-scale damage for all RMs. Other conventions are as in Table 1.

RM mesocyclone strength	EF0 (4066)	EF1 (2292)	EF2 (892)	EF3 (330)	EF4+ (89)
Weak	1767 (**0.435**)	659 (**0.288**)	93 (*0.104*)	6 (0.018)	0 (0.000)
Moderate	1143 (**0.281**)	651 (**0.284**)	167 (*0.187*)	26 (0.079)	2 (0.022)
Strong	1156 (**0.284**)	982 (**0.428**)	632 (***0.709***)	298 (***0.903***)	87 (***0.978***)

specified mode categories. A number of challenges were encountered in the process of identifying convective modes with severe thunderstorm and tornado events. Unambiguous discrimination between clusters and lines, as well as closely spaced cells versus clusters, was not always possible. However, the general subject of mode classification has rarely been discussed in any detail in the literature, and the challenges associated with this process can have a large impact on the resultant findings (e.g., KS10). A considerable number of events, particularly in the cool season, featured mixed modes or evolutions from one mode to another (e.g., line RM to QLCS) during the course of a series of events. The following cases illustrate the complexity that can occur relatively closely in time and space. Snapshots from the 15 November 2005 tornado outbreak show a view of different convective modes including a discrete RM that was rated as a category 4 event on the enhanced Fujita scale (EF4), cluster RM, EF2 line RM, and, finally, an EF0 QLCS across the lower Ohio and Tennessee Valleys (Figs. 3a,b). Arguably more complicated storm evolution patterns existed in another case (Figs. 3c,d) during the latter stages of an initial discrete cell that acquired supercell status as a cluster RM on 24 August 2006 in central North Dakota. The RM was subsequently overtaken by a developing and eastward-moving QLCS that became a bow echo after merging with the decaying RM. The bow-echo comma head circulation resulted in an EF2 tornado and sigwind event. Meanwhile, approximately 80 km to the southeast of the bow echo, a predominately discrete RM transitioned to a cluster RM and produced an EF0 tornado.

a. Linear hybrid classification

The most difficult challenge in mode classification involved discrimination between QLCSs and line RMs. Many cases exhibited a mix of RM and QLCS structures, such that a single mode designation was not easily identified (Fig. 4). Specific problems involved identification of mesocyclones versus mesovortices in the linear convective systems. A typical mesocyclone extends through a substantial fraction of storm depth (Doswell and Burgess 1993), whereas QLCS mesovortices are relatively shallow and not clearly associated with other supercell structures (Trapp and Weisman 2003; Weisman and Trapp 2003). When differences between the circulation types were not clear after considering all volumetric radar data [e.g., reflectivity structures such as hook echoes and a bounded weak echo region (BWER) after Lemon (1977)], a case was labeled a linear hybrid. This was done after multiple examinations by the authors and other established experts in radar interpretation from the NWS Warning Decision Training Branch (WDTB).

A case illustrating this problem occurred during the early morning hours of 11 May 2008 across central and southeastern Georgia (Fig. 4). An initial large cluster of storms moving from Alabama into west-central Georgia included several cellular structures ahead of an east-southeastward-moving band of storms growing upscale into a QLCS. Storm mergers and complex interactions occurred across central Georgia as the QLCS surged southeastward over the next few hours, and this complex pattern of evolution served as a classic illustration of the gray area that can exist between line RMs and QLCSs. Full volumetric radar data were utilized in order to examine the vertical structure and continuity of features needed to differentiate between the line RM and QLCS mesovortices that were responsible for a swath of tornado and sigwind events. The development and continuation of storm features (e.g., circulations, deep echo overhang and shape, echo tops) aided in

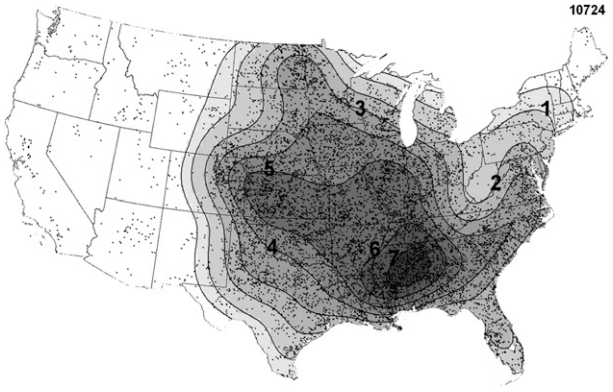

FIG. 6. Kernel density estimate on a 40 km × 40 km grid of all tornado events (EF0–EF5) assigned a convective mode. The minimum contour is 0.5 events per 10-yr estimate based on 2003–11 data. Labeled contours begin at 1 event per 10 yr. Black dots represent tornado events (10 724, labeled in the top right) that formed the basis of the kernel density estimate, and the color-fill scheme is gray scaled with heavier gray representing a higher tornado event estimate.

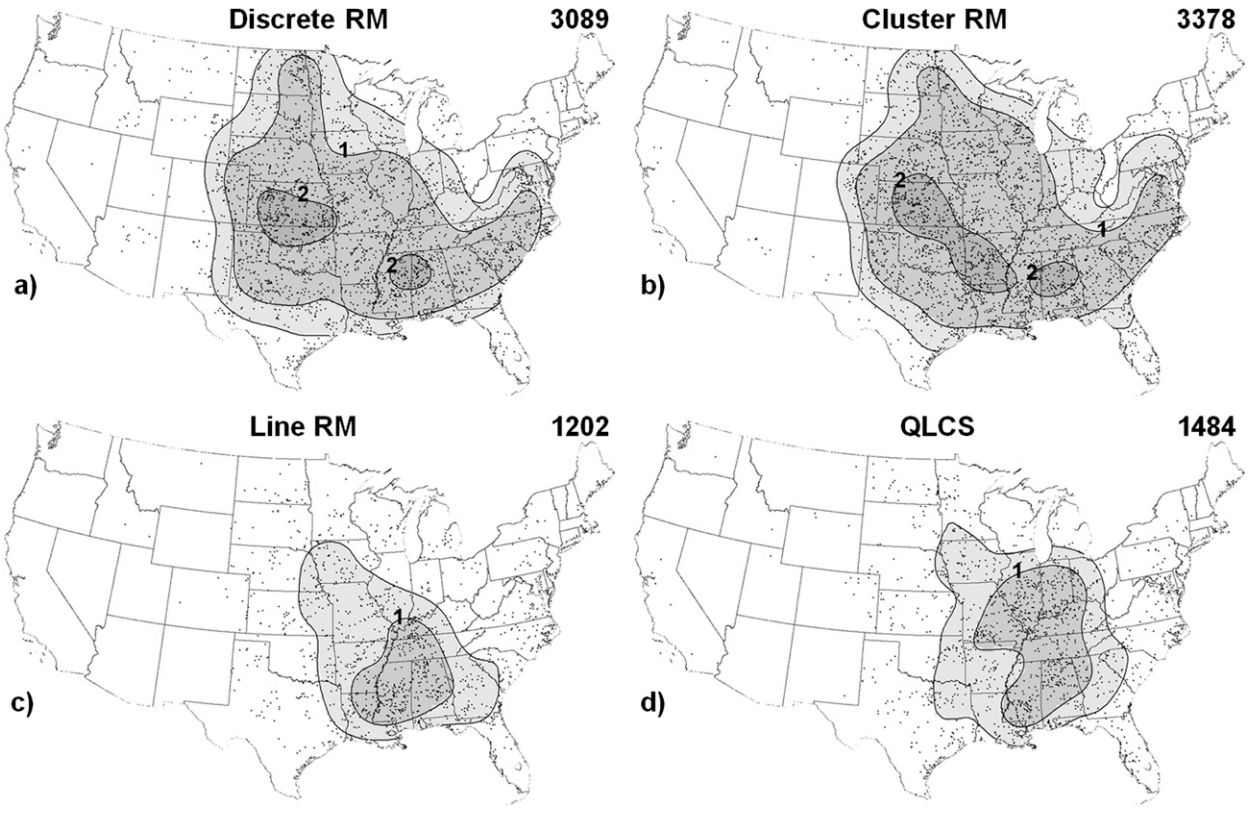

FIG. 7. As in Fig. 6, but for (a) discrete RM, (b) cluster RM, (c) line RM, and (d) QLCS convective modes.

mode assessment. The linear hybrid designation also acted as a descriptor to exemplify the uncertainty involved in classifying these cases.

b. *Effects of radar resolution on small supercells*

Other classification challenges involved storm size and the ability of WSR-88D data to resolve supercell structures. Storm depth and rotation were quite shallow in some tropical cyclone and cool season events compared to the larger spatial dimensions of storms in warm season Great Plains events. In some cases, rotation and storm depth did not exceed 3000 ft (0.91 km) and 20 000 ft (6.10 km) AGL, respectively. Because of the weaker rotational velocities observed with a small number of these cases, they were at times designated as a marginal supercell, which may be caused by the inability of the radar to resolve sufficient storm-scale rotation (e.g., horizontal range limitations) typical of a supercell based on the WDTB nomograms used in this study.

c. *Storm evolution*

Animation of multiple volumetric radar scans was needed in some instances to differentiate between subtle differences when several convective modes (e.g., QLCS and line RM) were in proximity to one another (i.e., $\leq$10 km and 5 min). This required intensive radar interrogation that in some cases was not sufficient to classify the event unambiguously. In those few circumstances, observable features (e.g., mesocyclones) in reflectivity and velocity data were tracked across multiple volume scans. An overwhelming majority of these cases were initially discrete RMs or cluster RMs that were overtaken by a QLCS, and moved in concert with the QLCS. Variability existed in how long a line RM would survive within a larger QLCS, ranging from a few minutes to 30 min or more. A relatively large portion of these cases continued to exhibit RM characteristics after the storm merger, with mesocyclone demise often coincident with the loss of appreciable cellular reflectivity structure. Once the initial circulation weakened below minimal mesocyclone strength and often concurrent with it, becoming indistinguishable from the QLCS velocity field, subsequent severe events in proximity to the original storm were attributed to the QLCS, despite any lingering cellular characteristics noted in reflectivity. Cases where a circulation later restrengthened, near the prior location of a line RM mesocyclone, were usually characterized as QLCS events. Given the highly variable nature of line RM demise in merger cases, an arbitrary cutoff of 15 min was applied for a few cases in which

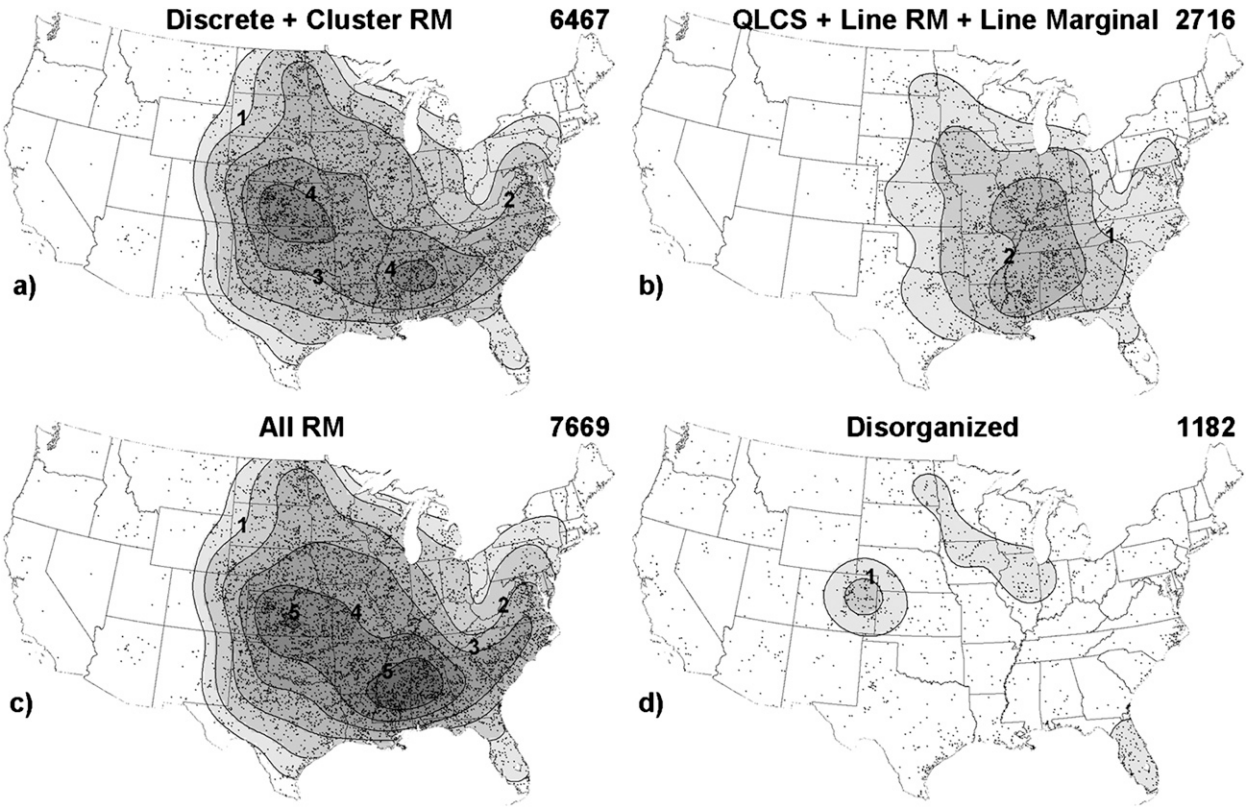

FIG. 8. As in Fig. 7, but for (a) discrete RM + cluster RM, (b) QLCS + line RM + line marginal, (c) all RM, and (d) disorganized convective modes.

radar evidence of supercell mesocyclone demise became uncertain because of radar horizontal range limitations. Trends in storm-scale circulations, echo-top character, and deeper reflectivity cores aided in assessing storm mode changes.

There were other situations where transient deeper reflectivity cores developed within a QLCS that evolved into a line RM. This was most common across the lower Mississippi Valley during the cool season. One example of this is a tornado and sigwind event over central Mississippi on 10 December 2008. A cursory glance at lowest tilt of base reflectivity from the Jackson, Mississippi (KDGX), radar shows seemingly innocuous QLCS structure around the time of the tornado and sigwind events (Figs. 5a and 5b). However, an examination of higher tilts of reflectivity and velocity shows a deep mesocyclone within a substantially deeper reflectivity core, along with higher echo tops (Figs. 5c and 5d). This case demonstrates the subtlety of proper convective mode classification that can require the examination of multiple radar tilts (Imy et al. 1992).

In summary, the application of the classification scheme presented is not entirely unambiguous, and there were a number of events that required very detailed and intensive examination to identify the most representative mode. However, the majority of the cases were straightforward to classify with a high degree of certainty. Furthermore, very large event sample sizes and a mix of convective mode examinations by multiple analysts likely minimizes the influence of individual biases and lends confidence to the results presented herein.

4. Results

a. Statistical distributions of events by mode

The distribution of tornado, sighail, and sigwind events by the convective mode is listed in Table 1. Tornadoes[2] were much more common with discrete and cluster RMs compared to QLCSs and disorganized modes, with RMs accounting for more than 71% of tornadoes. More strikingly, sighail events were produced almost exclusively by RMs and LMs. Conversely, sigwind events were

[2] We refer to EF-scale damage ratings for all tornadoes, though the enhanced Fujita scale was not implemented until February 2007. The F-scale tornado damage ratings in prior years correspond to the same numerical rating on the EF scale for the same type of damage, though the EF scale includes more specific damage indicators.

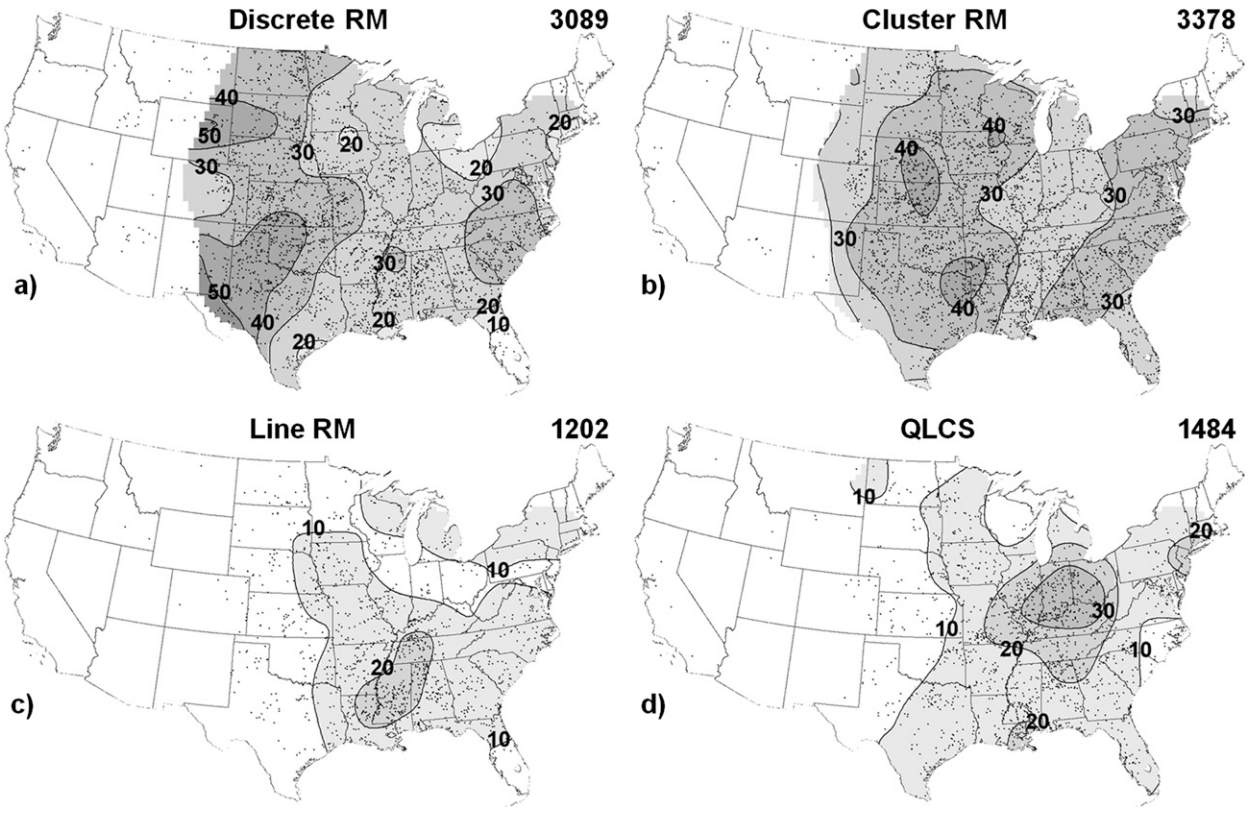

FIG. 9. Kernel density estimate on a 40 km × 40 km grid of (a) discrete RM, (b) cluster RM, (c) line RM, and (d) QLCS tornado event (EF0–EF5) percentage compared to all tornado events (2003–11), with 10% contour intervals labeled (black lines). Other conventions are the same as in Fig. 6.

more evenly distributed among supercells, QLCSs, and disorganized convective modes. Thus, without consideration of environmental information, sigwind clearly presents the greatest challenge to forecasters given the wide variety of convective modes capable of producing these events. A more detailed look at the tornado events reveals that discrete and cluster RMs were most commonly associated with the significant (EF2+ damage) tornadoes (Table 2), while nearly all EF3+ tornadoes were produced by some form of supercell. Like T05, our results indicate that EF1+ tornadoes are reported more frequently with QLCS convective modes compared to the total sample of tornado events, and that QLCS EF0 tornadoes are likely underreported.

All RM tornado events included categorical estimates of mesocyclone strength. Weak mesocyclones were most common with weak (EF0–EF1) tornadoes (Table 3), while EF3+ tornadoes were associated almost exclusively with strong mesocyclones. These findings are consistent across all three classes of RMs (discrete, cluster, or line), even though discrete and cluster RM tornadoes outnumbered line RM tornadoes by roughly a factor of 3 to 1. Thus, variations in tornado damage ratings were more closely related to mesocyclone strength than the specific type of RM.

b. *Spatial distributions of events by mode*

Since no sample size filter was applied to the kernel density estimates, the most plausible patterns likely exist in areas that have high numbers of events and are away from the edge of the domain. Caution should be noted in interpreting spatial estimation details near the edges of the domain that are presented in the next sections. Some slight underestimate of values within these regions is due to the lack of data over adjacent coastal waters and Canada/Mexico. Additionally, care should be taken in interpreting patterns in locations where only a small number of events control the resulting smoothed estimate (Fig. 1). With these considerations in mind, some important spatial signals in the relationship between tornado events and convective mode are revealed.

1) TORNADO OCCURRENCE BY MODE

The kernel density estimate provides a smooth field of the event and mode occurrence on the 40-km analysis

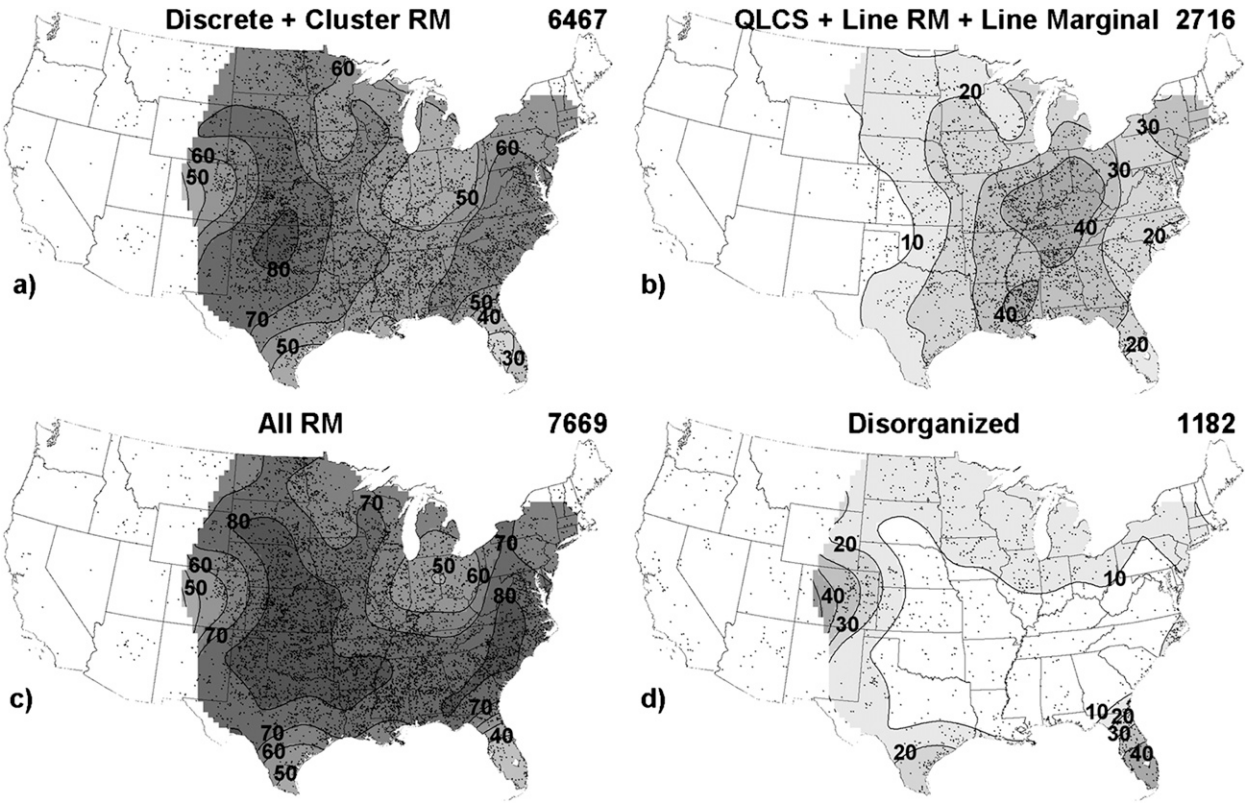

FIG. 10. As in Fig. 9, but for (a) discrete RM + cluster RM, (b) QLCS + line RM + line marginal, (c) all RM, and (d) disorganized convective modes.

grid. For example, an estimate for tornado event occurrence linearly extrapolated to 10 yr based on the 2003–11 dataset shows much of the area east of the Rockies, excluding the northeastern states, exceeded one tornado event per 10 yr on the 40-km grid (Fig. 6). The tornado event rate of occurrence estimate is highest from the central Great Plains eastward to the middle Mississippi Valley and south to Mississippi and Alabama [the so-called Dixie Alley; Gagan et al. (2010); Dixon et al. (2011)], where one tornado event is estimated every other year within a 1600 km^2 area, or about the size of a typical county in southeastern Kansas.

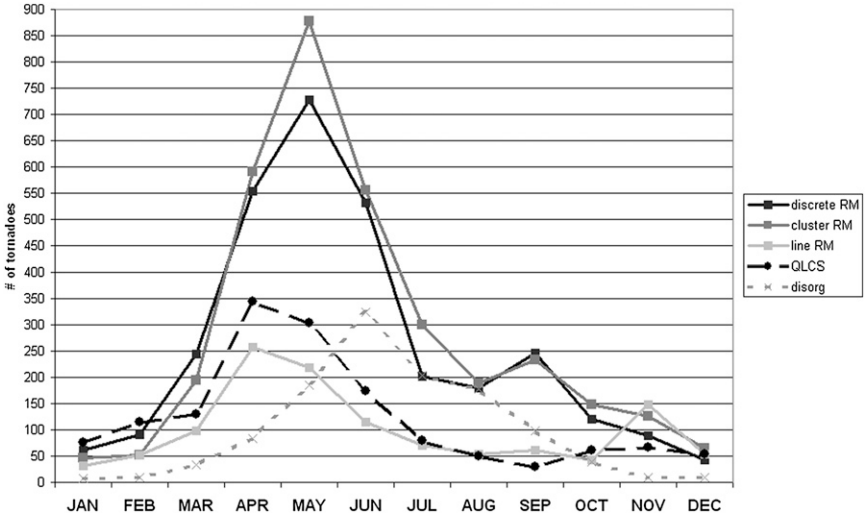

FIG. 11. Total number of tornado events by convective mode and month.

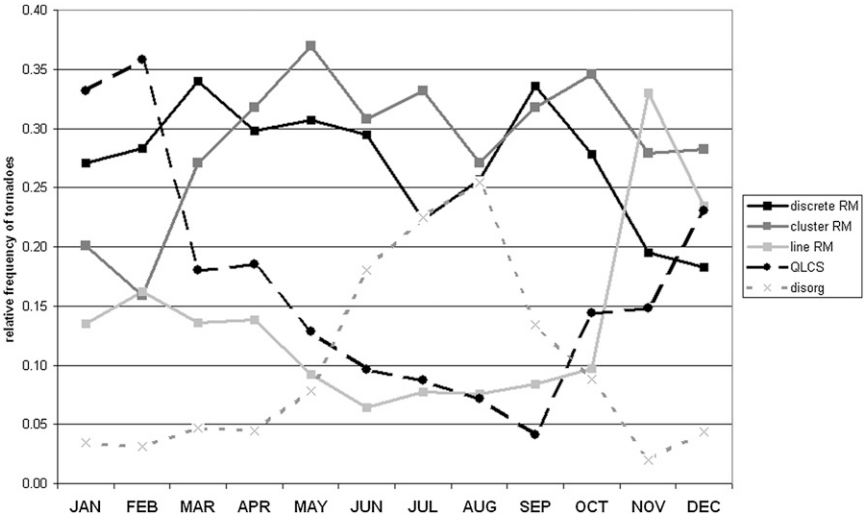

FIG. 12. Relative frequency of tornado events by convective mode and month. Monthly frequencies do not sum to one because tornadoes with marginal RMs and LMs are not plotted, but those events are included in the relative frequency calculations.

The highest estimated tornado event rate of occurrence for discrete RMs is located over the central Great Plains and portions of Mississippi and Alabama (Fig. 7a). Lower values are shown farther east toward the spine of the Appalachians and the mid-Atlantic region. A similar spatial distribution for cluster RMs is also evident (Fig. 7b). In contrast, the line RM maximum is located farther east of the Great Plains in the lower Mississippi

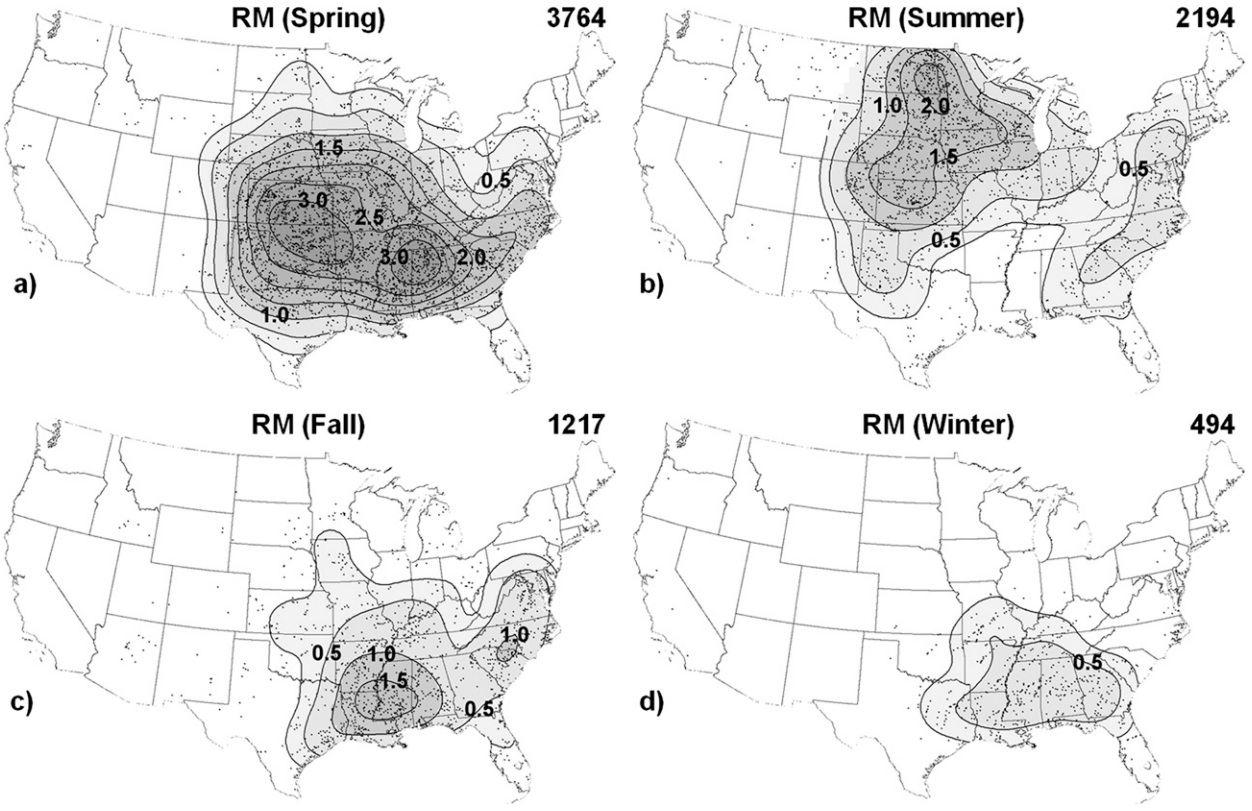

FIG. 13. All RM tornado events by season (a) March–May (spring), (b) June–August (summer), (c) September–November (fall), and (d) December–February (winter). The minimum contour is 0.25 events per 10-yr estimate based on 2003–11 data. Labeled contours begin at 0.5 events per 10 yr. Other conventions are the same as in Fig. 6.

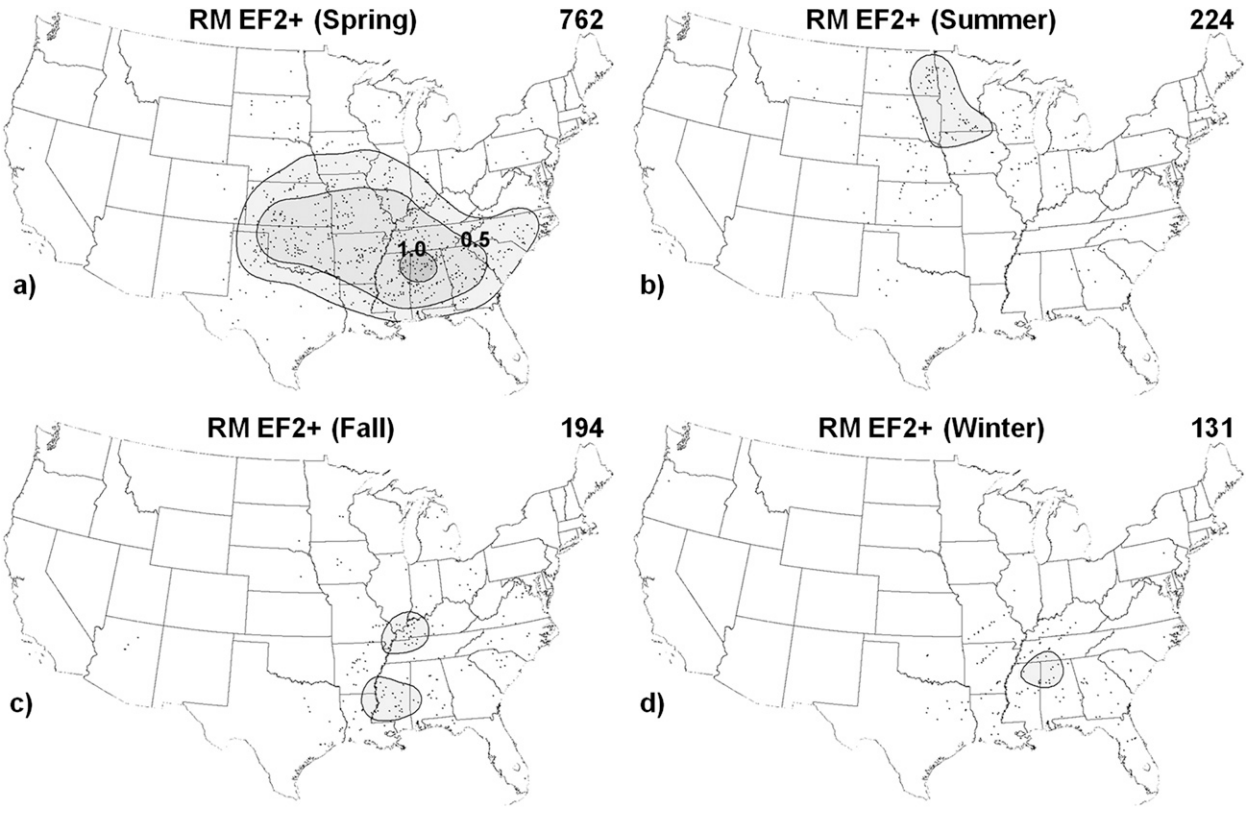

FIG. 14. As in Fig. 13, but for all RM EF2–EF5 tornado events.

Valley northward to the lower Ohio Valley (Fig. 7c). A comparable distribution to line RMs exists for QLCS, with a greater estimated rate of occurrence east of the Great Plains, from Mississippi and Alabama northward into the middle Mississippi Valley and lower Ohio Valley (Fig. 7d).

Differences between the organized cellular (discrete RM + cluster RM) and linear (QLCS + line RM + line marginal) convective modes with tornadoes are summarized by Fig. 8. The greatest estimated rate of occurrence for the organized cellular tornado events is located over the central Great Plains, with a corridor of high values extending southeastward into Mississippi and Alabama (Fig. 8a). A distinctly different distribution is found for the linear mode tornado events. These events were concentrated over the lower Ohio River valley and middle Mississippi River valley southward to the northern Gulf coast states (Fig. 8b), and exhibit a lower frequency compared to organized cellular tornadoes. Finally, comparisons can be made between all RMs (i.e., discrete + cluster + line) (Fig. 8c), QLCS (Fig. 7d), and disorganized (Fig. 8d) storm modes. Tornado events from RMs are most concentrated from the Great Plains eastward into the middle and lower Mississippi Valley and extending into the Carolina Piedmont. Tornado events from disorganized cells or clusters were relatively uncommon across the same areas dominated by supercells, except for parts of the Midwest, central high plains [i.e., the Denver convergence vorticity zone described in Brady and Szoke (1989)], and the Florida peninsula, which is largely attributable to diurnal sea-breeze thunderstorms and boundary interactions during the summer (Collins et al. 2000).

2) TORNADO RELATIVE FREQUENCY BY MODE

Additional convective mode spatial distribution information can be extracted through storm mode relative frequency, resulting in a proportional breakdown by convective mode. Discrete RMs were proportionally most common (≥40%) compared to other convective mode tornado events across a sizable portion of the northern high plains, as well as the southern high plains into the western half of Oklahoma (Fig. 9a). A slight eastward shift and lower relative frequency for cluster RMs (Fig. 9b) is apparent in the central and eastern Great Plains, with a secondary maximum over large parts of the eastern CONUS. A relative minimum corridor is noted in the lower Mississippi and Ohio Valleys, which corresponds to a higher relative frequency of line RMs (Fig. 9c) in the lower Mississippi and Tennessee

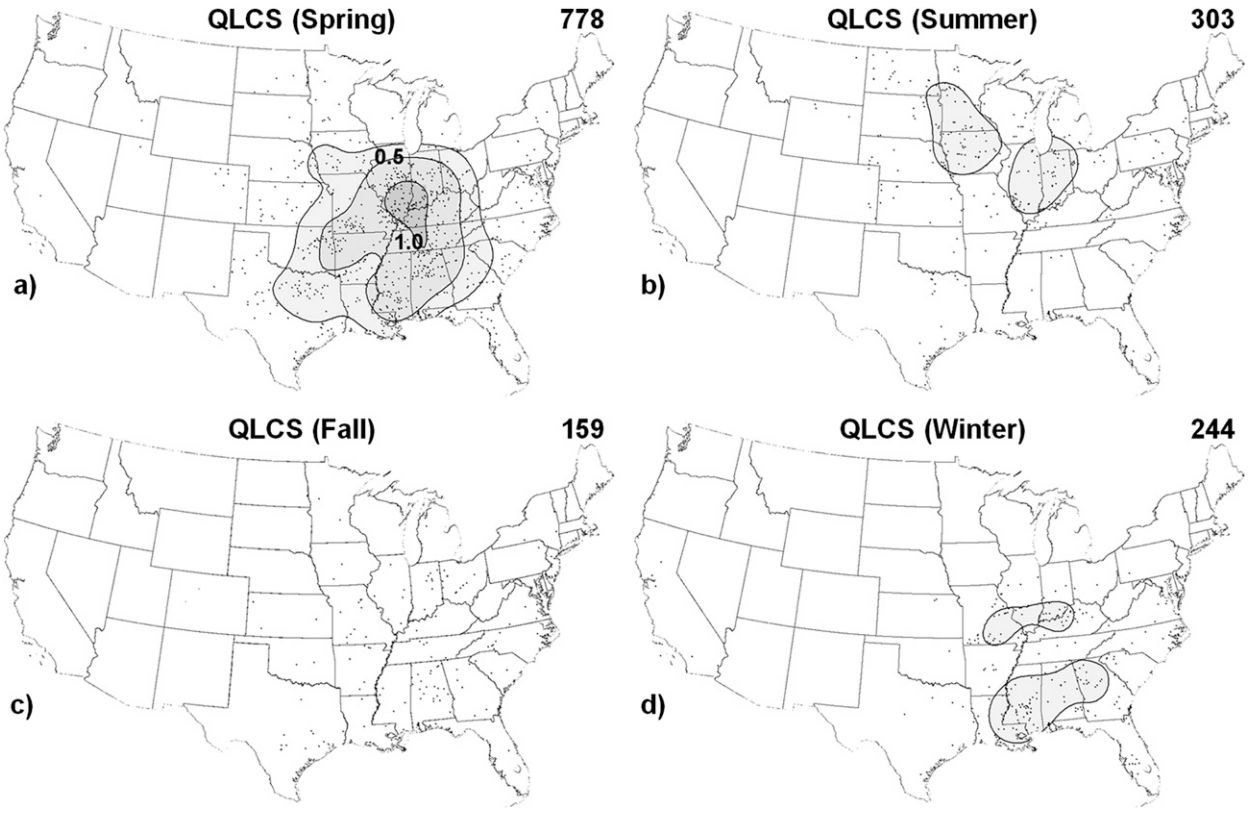

FIG. 15. As in Fig. 13, but for QLCS tornado events.

Valleys, and QLCS across the Ohio Valley (Fig. 9d). A sum of the discrete and cluster RMs (Fig. 10a) yields a pronounced bimodal spatial distribution with a maximum relative frequency of tornado events (in excess of 80%) centered over western Oklahoma. A distinct tendency for a higher proportion of tornado events resulting from linear convective modes is shown in Fig. 10b from the Ohio Valley southward to the lower Mississippi Valley. Tornado events were proportionally dominated by all RMs (Fig. 10c) across the Great Plains and Southeast, with RMs contributing less to tornado event frequencies in the Ohio Valley and southern Great Lakes. At least one-third of tornado events near the Colorado Front Range and the southern half of the Florida peninsula were from disorganized cells or clusters (Fig. 10d).

3) SEASONAL SPATIAL DISTRIBUTION BY MODE

Tornado events with discrete and cluster RMs clearly peak in May (Fig. 11), with a secondary peak in September related to tropical cyclones (Part III). The linear convective modes also peak in the spring (March–May), although at a substantially reduced rate of occurrence compared to the discrete and cluster RM tornadoes, and decrease from spring to summer (June–August). Tornadoes with disorganized convective modes (discrete nonsupercells and clusters) reach a maximum during the summer, with very few events during the late fall (September–November) and winter (December–February). When the absolute tornado mode frequency is examined by month, it is seen that the winter frequencies of tornado events pale in comparison to the spring. However, tornadoes with linear convective modes were *nearly* as frequent during the late fall and winter as discrete or cluster RMs (Fig. 12). The discrete and cluster RMs account for roughly 50%–70% of all tornadoes events throughout the year, whereas the linear convective modes approach a relative frequency near 50% only from November to February.

The kernel density estimates shown in Fig. 13 highlight the degree of spatial clustering for RM tornadoes by season. The absolute tornado counts vary substantially by season, with many more tornado events in the spring (Fig. 13a) compared to the winter (Fig. 13d). RM tornado events were most common across the interior northern Gulf coast during the winter, with the most frequent areas expanding from the Deep South northwestward into the central Great Plains during the spring, northward into the northern Great Plains and Midwest during the summer, and then back southward into the lower Mississippi Valley during the fall, similar

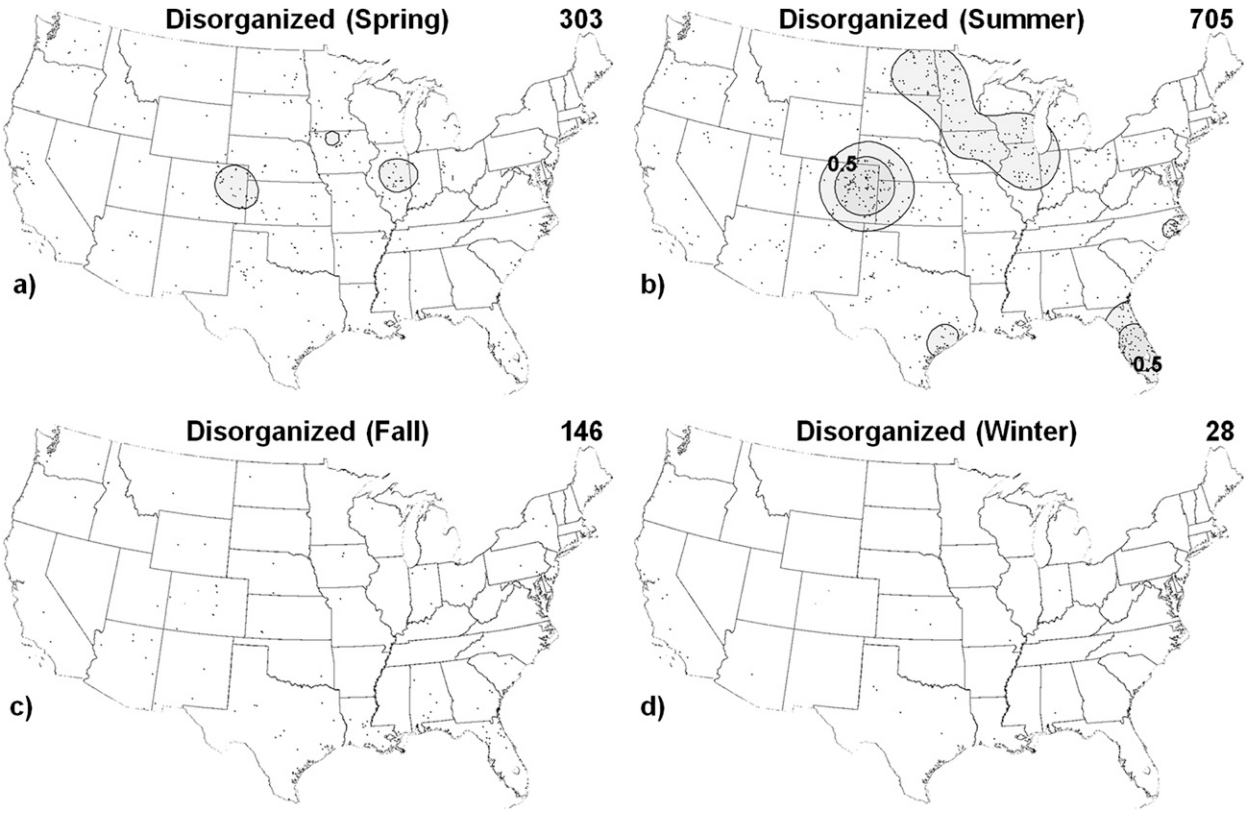

FIG. 16. As in Fig. 13, but for disorganized tornado events.

to the seasonal spatial shift in the annual tornado threat displayed in Brooks et al. (2003). During the late summer and early fall, a secondary maximum corridor is evident across the mid-Atlantic and Southeast regions and is largely attributed to multiple tropical cyclone tornado events in 2004 and 2005 (Part III). The significant tornado events (EF2–EF5 damage) with all RMs (Fig. 14) show a similar seasonal distribution when compared to all tornadoes, except for the northward extension from the lower Mississippi Valley toward the lower Ohio Valley in the fall. The rate of occurrence of sigtor RMs was about one-sixth the rate of occurrence of all RM tornadoes.

Compared to RMs during the spring and summer, the QLCS tornado events displayed a notable eastward shift away from the Great Plains toward the Mississippi and Ohio Valleys (Fig. 15), as discussed previously. The distribution of disorganized tornado events (Fig. 16) varies substantially from both the RM and QLCS tornado events by season. Local maxima in relative frequency are apparent across eastern Colorado and the upper Midwest during summer. The relative frequency of disorganized convective modes is also large across Florida in the summer, where diurnal convection is common with local sea-breeze circulations. Some of the disorganized mode tornado events along the Gulf coast in the fall were related to tropical cyclone landfalls, when supercell structures were not apparent with some cellular storms. Similar to the central valley of California during the winter, some of these tropical cyclone tornadoes may have been produced by supercells that were too small to be resolved by the WSR-88D.

As indicated in Table 1, nearly all sighail events occurred with discrete and cluster RMs and LMs. The

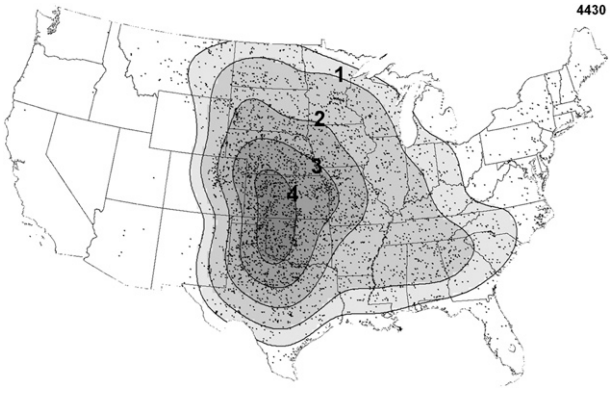

FIG. 17. As in Fig. 6, but for all supercell sighail events (includes both RMs and LMs).

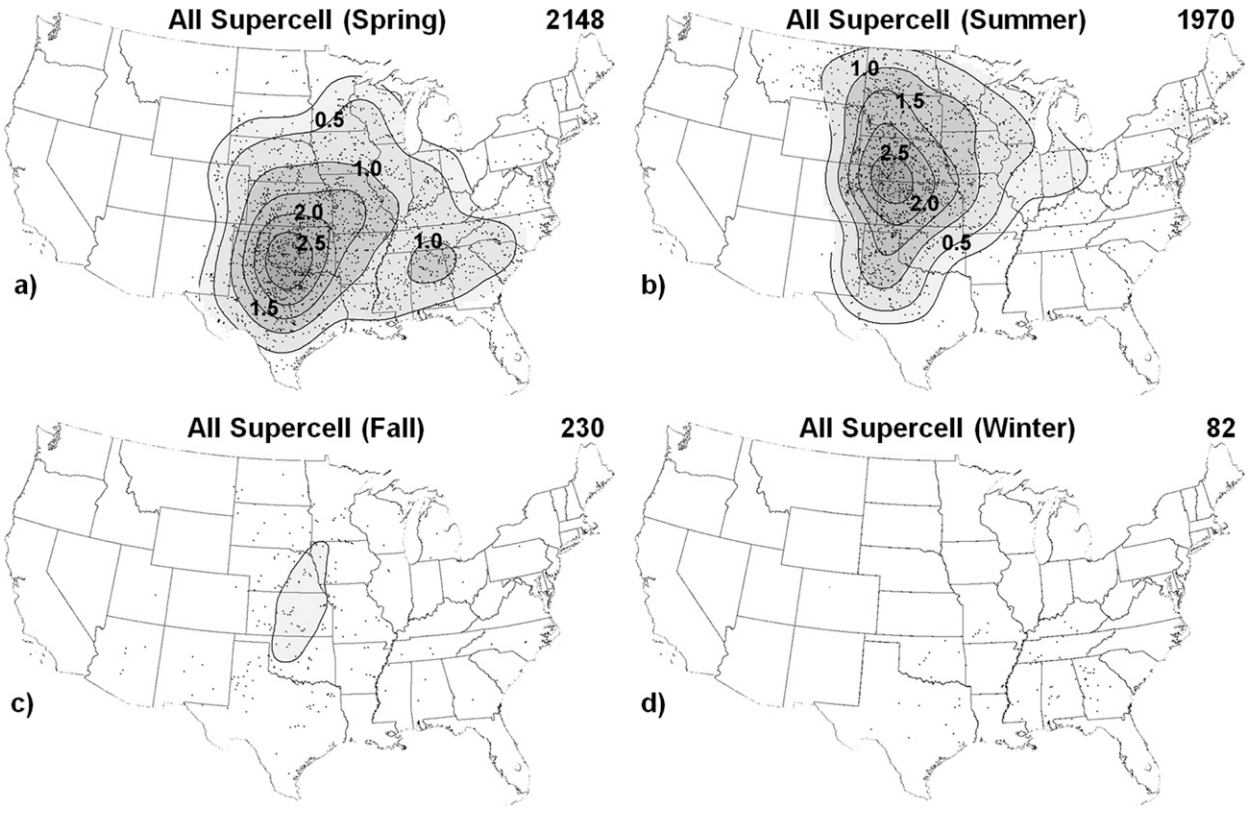

FIG. 18. As in Fig. 13, but for all supercell sighail events (includes both RMs and LMs).

spatial distribution of supercell sighail events is shown in Fig. 17, revealing the high-frequency axis over the Great Plains. From a seasonal perspective, the sighail events show a clear preference for the Great Plains during the spring and summer (Fig. 18), with the greatest frequency of sighail events displaced to the south of the maxima in RM tornado events (cf. Fig. 13) for the same seasons. The fall sighail distribution also favors the Great Plains compared to the lower Mississippi Valley for RM tornadoes, but the sample size for fall sighail events is much smaller and confined largely to September.

The sigwind estimated rate of occurrence exhibits several irregular maxima (Fig. 19), in stark contrast to the sighail events (Fig. 17). There may be several nonmeteorological explanations (see Weiss et al. 2002) for the irregular maxima across portions of the southern Appalachians and central Mississippi. Even with the kernel density smoothing, the authors' confidence in the depicted sigwind patterns is lower compared to both the sighail and tornado distributions, since a majority of sigwind events were estimates rather than measured anemometer wind gusts, and are without the benefit of a solid frame of reference (e.g., the comparison of hail to common objects of known diameter). Sigwind events from RMs (Fig. 20) were distributed similarly to RM tornadoes (Fig. 13) during the winter, spring, and summer. Summer QLCS sigwind events (Fig. 21) resembled the pattern of northwest flow severe weather outbreaks depicted in Johns (1984) and Johns and Hirt (1987) across the northern Great Plains to the Midwest.

Disorganized sigwind events (Fig. 22) were concentrated in the summer from the central Great Plains eastward to the southern Appalachians, with a relative minimum within this corridor across the Mississippi Valley. The southern Appalachians relative maximum

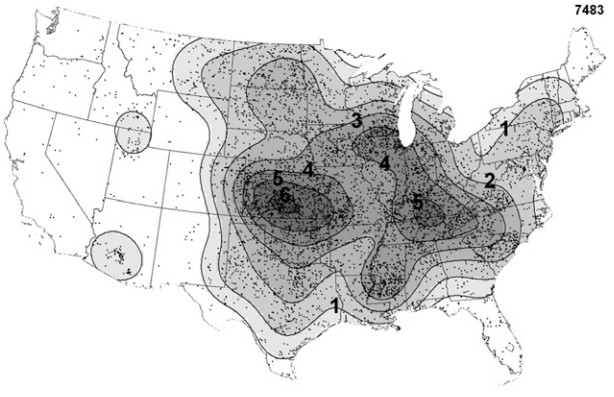

FIG. 19. As in Fig. 6, but for all sigwind events.

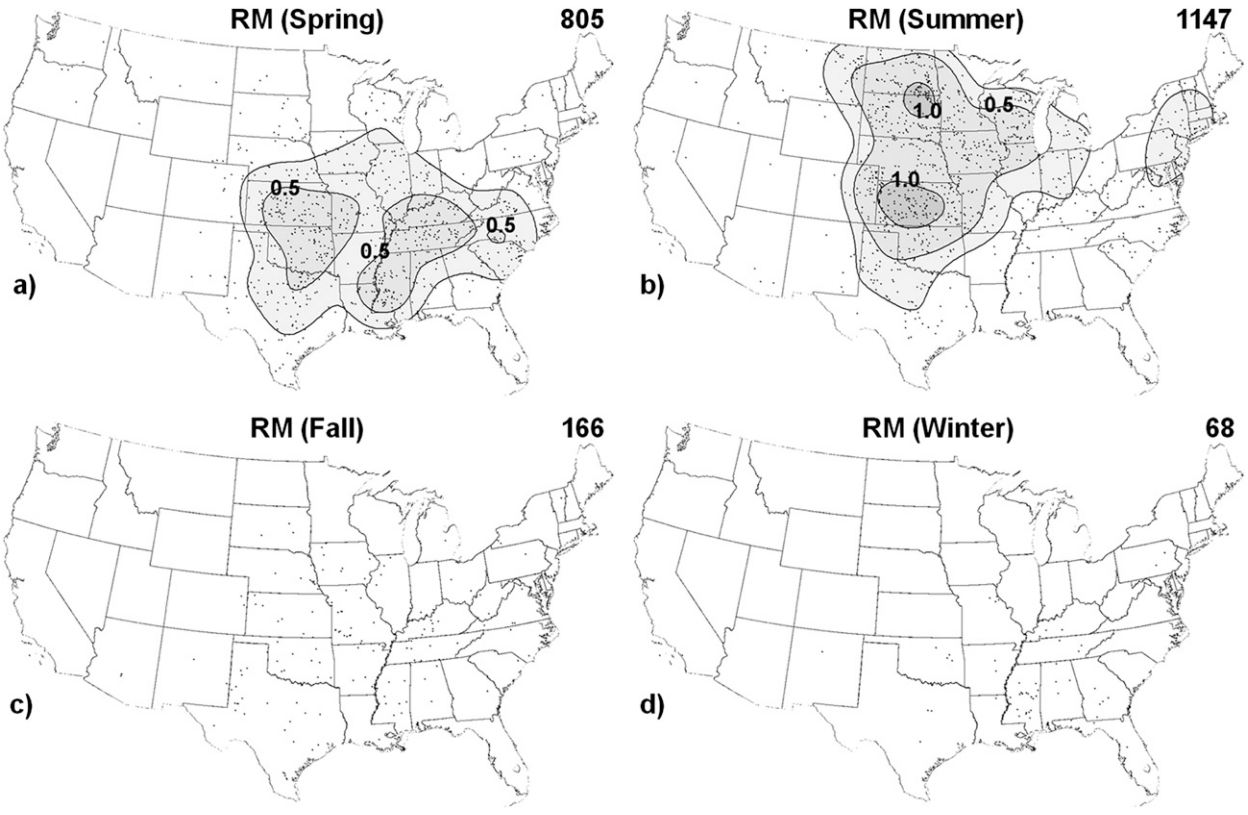

FIG. 20. As in Fig. 13, but for all RM sigwind events.

represents a substantial shift farther southeast than the RM and QLCS sigwind events (Figs. 20b, 21b, and 22b), and a large departure from the findings of Smith et al. (2010), where measured severe wind gusts (≥50 kt) were far more frequent in the Great Plains and Midwest compared to the southern Appalachians region. Interestingly, the disorganized sigwind events appear to be uncommon across the Gulf coast and Florida in the summer, despite the high frequency of diurnal thunderstorms. The localized clusters of events near Phoenix and Tucson, Arizona, and Salt Lake City, Utah, in the summer are likely related to local topography and increased density in population and/or observing systems compared to the other sparsely populated areas of the intermountain west. Small sample sizes preclude any substantial conclusions regarding the winter and fall sigwind distributions.

4) TEMPORAL DISTRIBUTION OF TORNADO EVENTS BY RADAR SITE

Tornado events within 230 km of the two WSR-88D sites exhibiting the greatest overall frequency of tornadoes in our sample [Dodge City, Kansas (KDDC), and KDGX] were chosen to examine the diurnal distribution of tornado events with the three major modes (supercell, QLCS, and disorganized). Tornado events were dominated by RMs at KDDC (Fig. 23), with a classic Great Plains temporal distribution from 2200 to 0300 UTC (late afternoon through evening). Tornadoes with QLCS or disorganized modes were much less common than RM tornadoes, but still tended to occur during the same portion of the day as the RM tornadoes. Conversely, KDGX (Fig. 24) reveals a much different distribution of tornado events by mode. Tornadoes with RMs occurred throughout the day and night, with more muted peaks around late afternoon and during the early morning. QLCS tornado events were much more common than at KDDC, and these QLCS events were distributed throughout the overnight and morning. Tornadoes with disorganized storms were rare within the coverage envelope of the KDGX radar site. These two sites represent only a small fraction of all tornado events across the CONUS, but Figs. 23 and 24 illustrate the potential for the development of convective mode climatologies for various radar sites.

5. Summary

Single-site, volumetric WSR-88D level II data were utilized to assign a convective mode for 22 901 tornado, sighail, and sigwind events, representing 78.5% of all

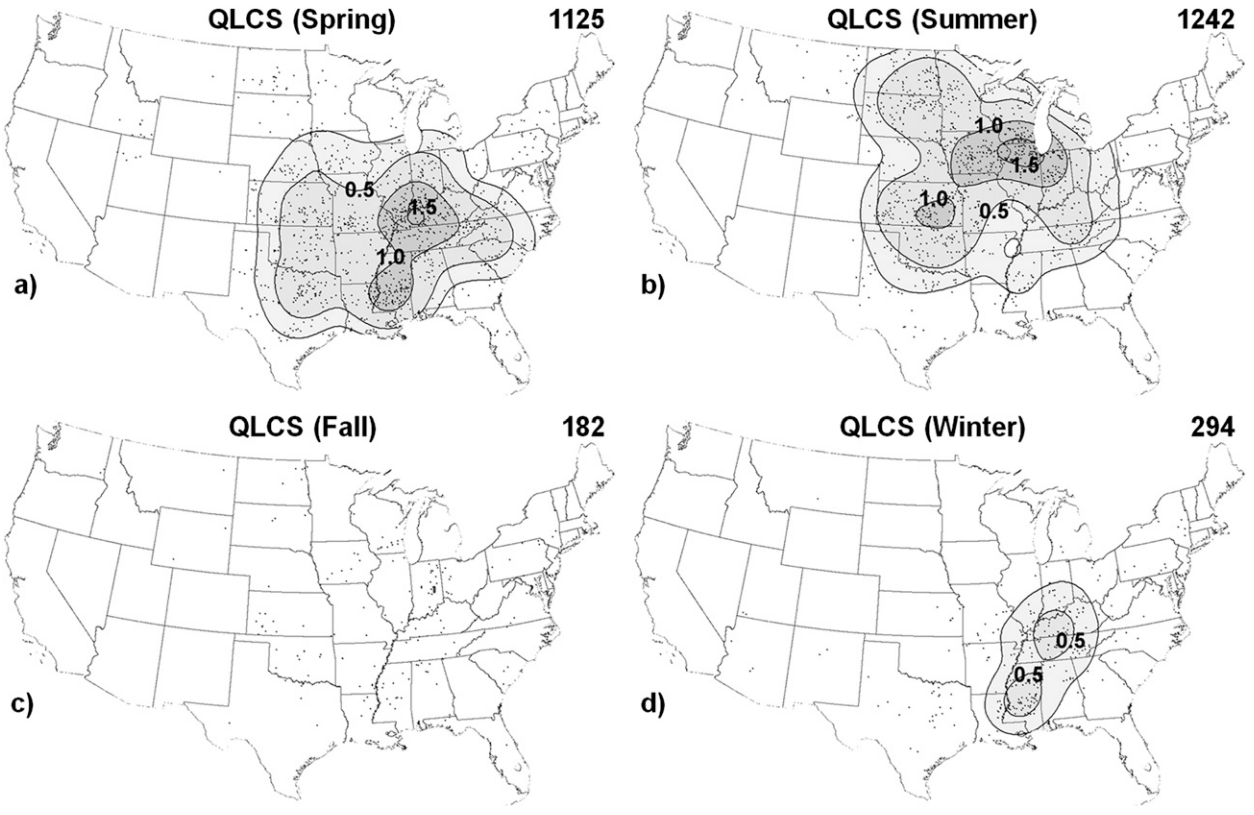

FIG. 21. As in Fig. 13, but for QLCS sigwind events.

such reported occurrences across the CONUS from 2003 to 2011. Three major categories of mode classification included QLCS, supercells, and disorganized. Subclassifications were also assigned: bow echo, discrete cell, cell in cluster, cell in line, cluster, and minor categories consisting of marginal supercell and linear hybrid. Although the majority of events were straightforward to classify, many event cases were very difficult to classify because of convective mode transitions; this presented many challenges in trying to bin the convective mode across a spectrum of storm types. A considerable number of events featured mixed modes, or evolution from one mode to another (e.g., line RM to QLCS), during a sequence of severe weather events. The most difficult challenge involved discrimination between QLCS and line RM. Many cases exhibited a mix of RM and QLCS structures, and such cases were noted as linear hybrids to convey a level of uncertainty in classification. Given the variations in convective mode classes used in previous studies, this work also highlights the need to develop a unified community convective mode classification scheme. This is necessary to uniformly describe the full spectrum of storm types, such that classification differences do not dominate the interpretation of atmospheric variables related to the various convective modes.

Although various degrees of uncertainty existed in subjectively classifying a convective mode, especially those with complex storm-scale evolutions that occurred near the time of a given event, the unprecedented sample size in this study likely overwhelms the uncertainty associated with any specific event mode designation. As such, the relative frequencies, along with spatial and temporal distributions, illustrate the important controlling influences convective mode has on the type of severe weather. The primary findings of this study are highlighted below:

- Discrete and cluster RMs were relatively more common as EF-scale damage ratings increased.
- Weak mesocyclones were most common with weak tornadoes, while 90% of EF3–EF5 tornadoes were associated with strong mesocyclones.
- Discrete RM tornado events were proportionally more common across the high plains, with a transition eastward to higher relative frequencies of tornadoes with linear convective modes across the Mississippi and Ohio Valleys.
- Tornado events from linear convective modes were nearly as frequent in the winter months as the sum of the discrete and cluster RM tornado events.

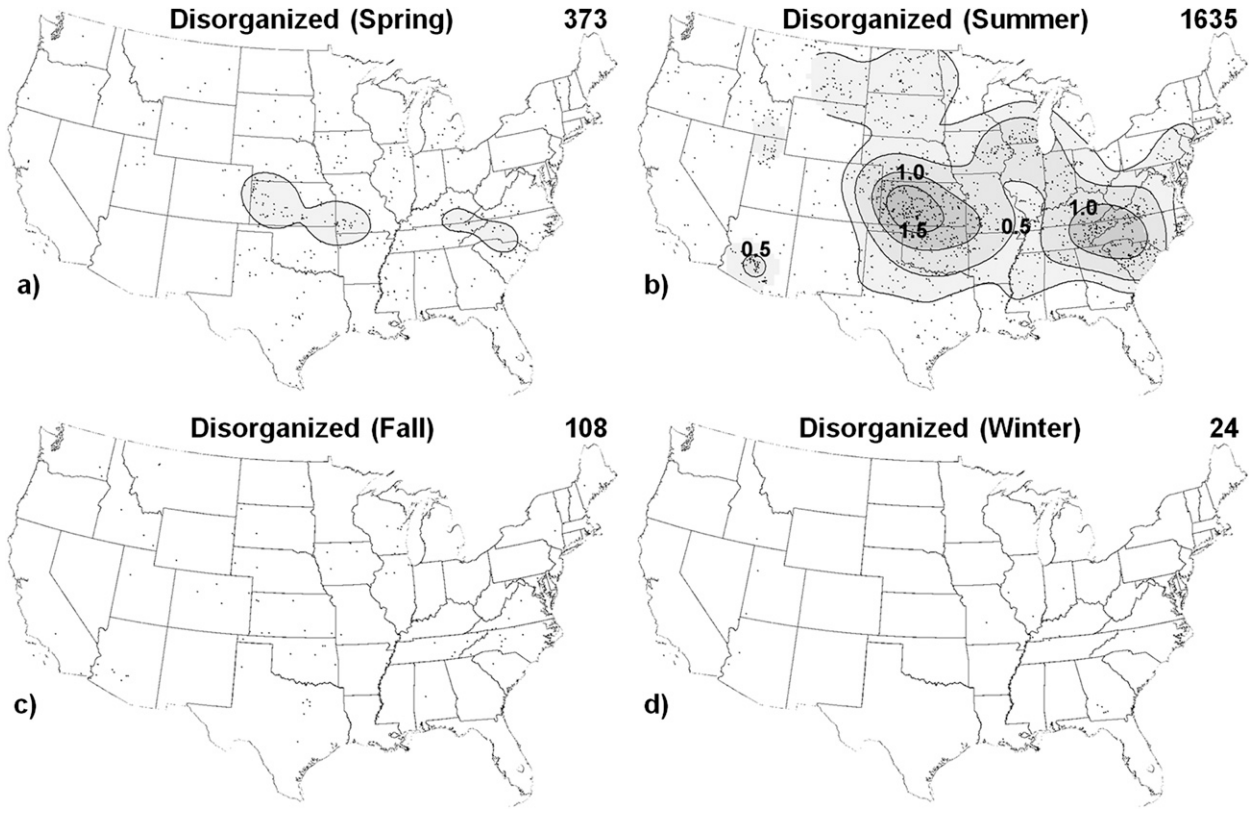

FIG. 22. As in Fig. 13, but for disorganized sigwind events.

- RM tornado events were most common across the interior northern Gulf coast during the winter, expanding across the Deep South and into the central Great Plains during the spring, northward into the northern Great Plains and Midwest during the summer, and then back southward into the lower Mississippi Valley during the fall.
- QLCS tornado events displayed a notable eastward displacement away from the Great Plains toward the Mississippi and Ohio Valleys during the spring and summer.

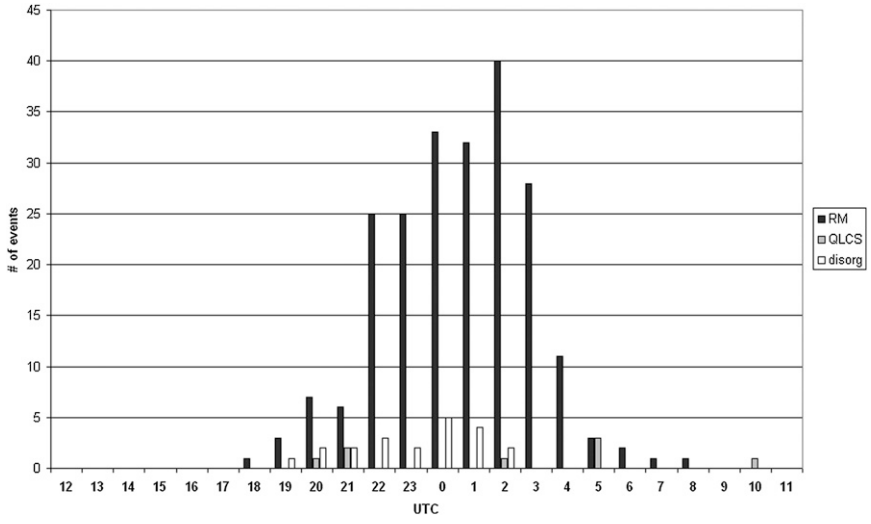

FIG. 23. Frequency of tornado events by hour and convective mode, for those closest to the KDDC WSR-88D site. Events were binned according to the hour of occurrence (e.g., 2045 UTC is listed here as 2000 UTC).

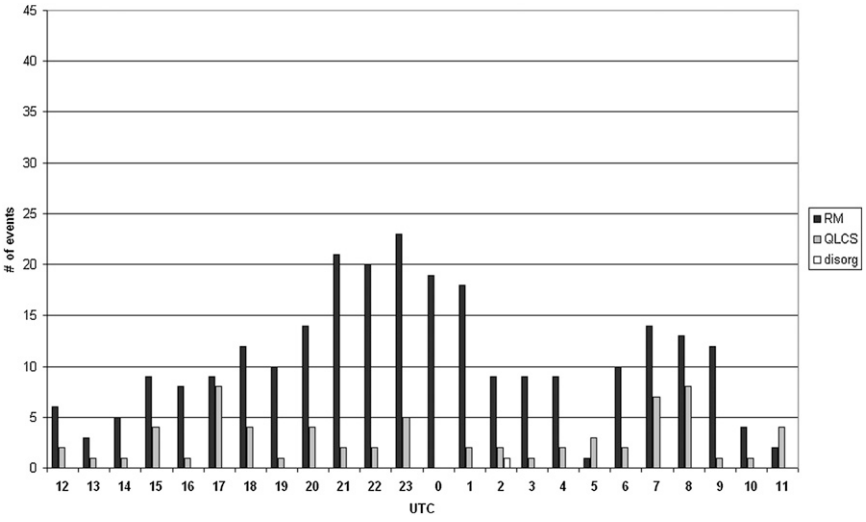

FIG. 24. As in Fig. 23, but for Jackson, MS.

The majority of tornadoes occurred with discrete and cluster RMs compared to the QLCS and disorganized modes. More than 95% of EF3–EF5 tornadoes and sighail events were produced by supercells. Conversely, sigwind events were more evenly distributed among the RM, QLCS, and disorganized convective modes. Thus, without consideration of environmental information, significant wind events clearly present the greatest challenge to forecasters given the wide variety of associated convective modes.

A monthly and seasonal breakdown revealed that tornado events with discrete and cluster RMs clearly peaked in May, with a secondary peak in September related to tropical cyclones. The linear convective modes of QLCS and line RM also peaked in the spring and decreased from May to July. Tornadoes with disorganized convective modes (discrete nonsupercells and clusters) reached a maximum during June and July, with very few events during the winter. Although the frequency of tornado events was substantially less during the winter compared to spring, winter tornadoes with linear convective modes were nearly as frequent as discrete or cluster RM events. From a forecasting perspective, this implies that May potentially can be a more predictable time of year for supercell tornadoes as a result of decreasing relative frequencies of QLCS tornadoes during winter and prior to increasing relative frequencies of disorganized convective modes during summer. However, this is dependent on utilizing techniques for discrimination between tornadic and nontornadic supercells.

Future work will include continued expansion of the database on a yearly basis, with the goal of providing a solid foundation for multifaceted forecast verification at the SPC. A more detailed investigation will be performed on tornadic storms by interrogating low-level circulation strength using superresolution lowest tilt velocity data, in order to examine the relationship between the convective mode, the EF scale, the near-storm environment, and circulation strength. As the dataset expands, the examination of diurnal trends for various convective modes and their associated near-storm environments by severe type, using a defined time period (e.g., hour, month), will be possible.

Acknowledgments. Andy Dean (SPC) provided valuable assistance in filtering the severe events and Jason Levit (NWS headquarters) laid the initial groundwork for filtering the severe events. David Cleaver (SPC) helped develop computer code to display some data in GIS. This work also benefitted from multiple discussions with Steven Weiss and Dr. Russell Schneider (SPC). The authors express their gratitude to Les Lemon, Jim LaDue, and Paul Schlatter of the Warning Decision Training Branch for reviewing and discussing our radar interpretation for several difficult convective mode cases. The thorough reviews by Matt Bunkers, Les Lemon, and one anonymous reviewer helped clarify and strengthen our presentation.

REFERENCES

Andra, D. L., Jr., 1997: The origin and evolution of the WSR-88D mesocyclone recognition nomogram. Preprints, *28th Conf. on Radar Meteorology,* Austin, TX, Amer. Meteor. Soc., 364–365.

Benjamin, S. G., and Coauthors, 2004: An hourly assimilation–forecast cycle: The RUC. *Mon. Wea. Rev.,* **132,** 495–518.

Bothwell, P. D., J. A. Hart, and R. L. Thompson, 2002: An integrated three-dimensional objective analysis scheme in use at the Storm Prediction Center. Preprints, *21st Conf. on Severe Local Storms,* San Antonio, TX, Amer. Meteor. Soc., JP3.1.

[Available online at https://ams.confex.com/ams/SLS_WAF_NWP/techprogram/paper_47482.htm.]

Brady, R. H., and E. J. Szoke, 1989: A case study of nonmesocyclone tornado development in northeast Colorado: Similarities to waterspout formation. *Mon. Wea. Rev.,* **117,** 843–856.

Brooks, H. E., C. A. Doswell III, and M. P. Kay, 2003: Climatological estimates for local daily tornado probability for the United States. *Wea. Forecasting,* **18,** 626–640.

Browning, K. A., 1964: Airflow and precipitation trajectories within severe local storms which travel to the right of the winds. *J. Atmos. Sci.,* **21,** 634–639.

Collins, W. G., C. H. Paxton, and J. H. Golden, 2000: The 12 July 1995 Pinellas County, Florida, tornado/waterspout. *Wea. Forecasting,* **15,** 122–134.

Crum, T. D., R. L. Alberty, and D. W. Burgess, 1993: Recording, archiving, and using WSR-88D data. *Bull. Amer. Meteor. Soc.,* **74,** 645–653.

Dixon, P. G., A. E. Mercer, J. Choi, and J. S. Allen, 2011: Tornado risk analysis: Is Dixie Alley an extension of Tornado Alley? *Bull. Amer. Meteor. Soc.,* **92,** 433–441.

Doswell, C. A., III, and D. W. Burgess, 1988: On some issues of United States tornado climatology. *Mon. Wea. Rev.,* **116,** 495–501.

——, and ——, 1993: Tornadoes and tornadic storms: A review of conceptual models. *The Tornado: Its Structure, Dynamics, Prediction, and Hazards, Geophys. Monogr.,* Vol. 79. Amer. Geophys. Union, 161–172..

——, H. E. Brooks, and M. P. Kay, 2005: Climatological estimates of daily local nontornadic severe thunderstorm probability for the United States. *Wea. Forecasting,* **20,** 577–595.

Duda, J. D., and W. A. Gallus Jr., 2010: Spring and summer midwestern severe weather reports in supercells compared to other morphologies. *Wea. Forecasting,* **25,** 190–206.

Edwards, R., A. R. Dean, R. L. Thompson, and B. T. Smith, 2012: Convective modes for significant severe thunderstorms in the contiguous United States. Part III: Tropical cyclone tornadoes. *Wea. Forecasting,* in press.

Fujita, T. T., 1978: Manual of downburst identification for project NIMROD. Satellite and Mesometeorology Research Paper 156, Dept. of Geophysical Sciences, University of Chicago, 104 pp.

Gagan, J. P., A. E. Gerard, and J. Gordon, 2010: A historical and statistical comparison of ''Tornado Alley'' to ''Dixie Alley.'' *Natl. Wea. Dig.,* **34** (2), 145–156.

Gallus, W. A., Jr., N. A. Snook, and E. V. Johnson, 2008: Spring and summer severe weather reports over the Midwest as a function of convective mode: A preliminary study. *Wea. Forecasting,* **23,** 101–113.

Grams, J. S., R. L. Thompson, D. V. Snively, J. A. Prentice, G. M. Hodges, and L. J. Reames, 2012: A climatology and comparison of parameters for significant tornado events in the United States. *Wea. Forecasting,* **27,** 106–123.

Hales, J. E., Jr., 1988: Improving the watch/warning program through use of significant event data. Preprints, *15th Conf. on Severe Local Storms,* Baltimore, MD, Amer. Meteor. Soc., 165–168.

Hocker, J. E., and J. B. Basara, 2008a: A 10-year spatial climatology of squall line storms across Oklahoma. *Int. J. Climatol.,* **28,** 765–775.

——, and ——, 2008b: A Geographic Information Systems–based analysis of supercells across Oklahoma from 1994 to 2003. *J. Appl. Meteor. Climatol.,* **47,** 1518–1538.

Imy, D. A., K. J. Pence, and C. A. Doswell III, 1992: On the need for volumetric radar data when issuing severe thunderstorm and tornado warnings. *Natl. Wea. Dig.,* **17** (4), 2–17.

Johns, R. H., 1984: A synoptic climatology of northwest-flow severe weather outbreaks. Part II: Meteorological parameters and synoptic patterns. *Mon. Wea. Rev.,* **112,** 449–464.

——, and W. D. Hirt, 1987: Derechos: Widespread convectively induced windstorms. *Wea. Forecasting,* **2,** 32–49.

Kis, A. K., and J. M. Straka, 2010: Nocturnal tornado climatology. *Wea. Forecasting,* **25,** 545–561.

Lemon, L. R., 1977: New severe thunderstorm radar identification techniques and warning criteria: A preliminary report. NOAA Tech. Memo. NWS NSSFC-1, 60 pp.

Schneider, R. S., and A. R. Dean, 2008: A comprehensive 5-year severe storm environment climatology for the continental United States. Preprints, *24th Conf. Severe Local Storms,* Savannah, GA, Amer. Meteor. Soc., 16A.4. [Available online at http://ams.confex.com/ams/pdfpapers/141748.pdf.]

Silverman, B. W., 1986: *Density Estimation for Statistics and Data Analysis*. Chapman and Hall, 177 pp.

Smith, B. T., J. L. Guyer, and A. R. Dean, 2008: The climatology, convective mode, and mesoscale environment of cool season severe thunderstorms in the Ohio and Tennessee Valleys, 1995–2006. Preprints, *24th Conf. Severe Local Storms,* Savannah, GA, Amer. Meteor. Soc., 13B.7. [Available online at http://ams.confex.com/ams/pdfpapers/141968.pdf.]

——, A. C. Winters, C. M. Mead, A. R. Dean, and T. E. Castellanos, 2010: Measured severe wind gust climatology of thunderstorms for the contiguous United States, 2003–2009. Preprints, *25th Conf. Severe Local Storms,* Denver, CO, Amer. Meteor. Soc., 16B.3. [Available online at http://ams.confex.com/ams/pdfpapers/175594.pdf.]

Stumpf, G. J., A. Witt, E. D. Mitchell, P. L. Spencer, J. T. Johnson, M. D. Eilts, K. W. Thomas, and D. W. Burgess, 1998: The National Severe Storms Laboratory mesocyclone detection algorithm for the WSR-88D. *Wea. Forecasting,* **13,** 304–326.

Thompson, R. L., R. Edwards, J. A. Hart, K. L. Elmore, and P. Markowski, 2003: Close proximity soundings within supercell environments obtained from the Rapid Update Cycle. *Wea. Forecasting,* **18,** 1243–1261.

——, B. T. Smith, J. S. Grams, A. R. Dean, and C. Broyles, 2012: Convective modes for significant severe thunderstorms in the contiguous United States. Part II: Supercell and QLCS tornado environments. *Wea. Forecasting,* **27,** 1136–1154.

Trapp, R. J., and M. L. Weisman, 2003: Low-level mesovortices within squall lines and bow echoes. Part II: Their genesis and implications. *Mon. Wea. Rev.,* **131,** 2804–2823.

——, S. A. Tessendorf, E. S. Godfrey, and H. E. Brooks, 2005: Tornadoes from squall lines and bow echoes. Part I: Climatological distribution. *Wea. Forecasting,* **20,** 23–34.

——, D. M. Wheatley, N. T. Atkins, R. W. Przybylinski, and R. Wolf, 2006: Buyer beware: Some words of caution on the use of severe wind reports in postevent assessment and research. *Wea. Forecasting,* **21,** 408–415.

Weisman, M. L., and R. J. Trapp, 2003: Low-level mesovortices within squall lines and bow echoes. Part I: Overview and dependence on environmental shear. *Mon. Wea. Rev.,* **131,** 2779–2803.

Weiss, S. J., J. A. Hart, and P. R. Janish, 2002: An examination of severe thunderstorm wind report climatology: 1970–1999. Preprints, *21st Conf. Severe Local Storms,* San Antonio, TX, Amer. Meteor. Soc., 446–449.